International Journal of Dynamics and Control (2024) 12:1679–1693
https://doi.org/10.1007/s40435-023-01298-z

Force and position coordination for delayed bilateral teleoperation of a manipulator robot

Diego D. Santiago[1] · Emanuel Slawiñski[1] · Lucio R. Salinas[1,2] · Vicente A. Mut[1]

Received: 10 April 2023 / Revised: 7 August 2023 / Accepted: 23 August 2023 / Published online: 21 September 2023

Abstract
This paper focuses on the design and analysis of a P+d+f (Proportional, Derivative, and Force) variable control strategy aimed at delayed bilateral teleoperation of a manipulator robot, the ultimate goal of which is to obtain simultaneous coordination of force and position between the haptic device and the robot. The proposed controller changes the damping based on both the time delay and feedback power signal measured online. Unlike other P+d+f strategies, this proposal avoids terms with discontinuities in the controller, cancellation of human and environment forces and also prevents the explicit use of environment parameters. The proposal uses variable damping dependent on a feedback power signal, which reduces kinetic energy to ensure bounded control errors. Simulations are performed to verify that dual coordination is achieved without using explicit nonlinear damping in the controller or needing the parametric knowledge of the environment model, which is useful to apply the controller to most commercial manipulator robots.

Keywords Bilateral teleoperation · Force–position coordination · Time delay · Transparency · Lyapunov–Krasovskii

1 Introduction

Teleoperation systems broaden human operators' capabilities allowing them to remotely perform physical work in places that may be too dangerous or even unreachable for humans [1]. They are formed by two stations connected by a communication link which inevitably introduces backward and forward time delay. The robot that performs the physical work is located in the remote station, which we call follower or remote robot. On the other hand, the robot that generates the commands is located in the local station, and we will refer to it as a haptic device or leader. A human operator uses the haptic device to drive the remote robot to complete a task while he or she receives multimedia information (visual and audio) and force feedback from the remote site. This coupling is defined in the literature as bilateral teleoperation and allows the human tactile perception of the remote task (closed-loop control). These systems can be applied to diverse fields such as rescue and surveillance, spatial and ground exploration, explosives deactivation, tele-manufacturing, among others [2].

Delayed bilateral teleoperation systems (DBTS) are modeled from delayed nonlinear multi-degree-of-freedom (DOF) robotic systems, where one main issue is the destabilizing effect caused by the time delay, which is time-varying and asymmetric [3–5]. Many controllers mostly proposed and evaluated using DBTS of robot arm manipulators were introduced. Some of these strategies have been modified, adapted, and tested using other types of remote robots such as wheeled mobile robots [6], mobile manipulators [7–9], UAV (unmanned aerial vehicles) [10, 11], and teleoperation networks [12, 13]. With respect to the stability of DBTS, the majority of the schemes use passivity-based control [14] including scattering transformation, wave variable and controllers based on time-domain passivity [15–17], damping injection [18] and adaptive, impedance and neural network

✉ Lucio R. Salinas
lucio.salinas@bristol.ac.uk

Diego D. Santiago
dsantiago@inaut.unsj.edu.ar

Emanuel Slawiñski
slawinski@inaut.unsj.edu.ar

Vicente A. Mut
vmut@inaut.unsj.edu.ar

[1] Instituto de Automática (INAUT), Universidad Nacional de San Juan (UNSJ) - CONICET, Avda. San Martín Oeste 1109, J5400ARL San Juan, Argentina

[2] Department of Engineering Mathematics, University of Bristol, Beacon House, Queens Road, Bristol BS8 1QU, UK

controllers [19, 20]. Other sources that induce non-passive behaviors in the system are the human operator and the environment [21]. To achieve stable position coordination, the simplest controller is the P+d type. In this type of controller, the energy extraction, based on damping, must be high enough to get stable position coordination [18, 22, 23]. But these controllers are calibrated mainly depending on the time delay and the setting is free of the human operator. Even more, the condition to reach stability is frequently fulfilled considering passive human actions represented by a spring-damping model [24]. However, this model type does not always faithfully represent the human operator behavior [21], and therefore, other models should be analyzed to get conclusions about how the controller could be designed or calibrated depending on them.

On the other hand, beyond stability, one of the crucial concepts in bilateral teleoperation is known as transparency, defined in [25] as a measure of how the human is coupled to the remote environment. In any bilateral teleoperator system design, the essential goal is to provide an adequate transmission of signals (positions, velocities, forces) to link the operator as closely as possible to the remote workspace. If the teleoperation system is completely transparent, then operators should feel a direct interaction with the remote task. Usually, there is a balance between stability and transparency. In [26], the transparency definition is quantitative extended to the time domain, isolating three components called remote, local, and instantaneous.

With the intention of achieving stable and transparent systems, different architectures have been proposed; the firstly called four-channel architectures which send a bidirectional flow of force and position, such as position–force domain passivity schemes, based mainly on experimental study and showing that the human operator does not remain passive in the position–force domain for all ranges of frequencies [27], TDPA (time-domain passivity approach) which combines passivity observers and passivity controllers [28–31] where these schemes can be included into a two-layer approach as in [32] but the main drawback of the schemes TDPA are that they need the whole energy flow which cannot be computed on one side of the teleoperation system and therefore predictors or delayed energy flow are necessary to use, and Lyapunov-based strategies addressed to achieve simultaneous tracking of force and position as in [33, 34], where P+d controllers plus force transmission (P+d+f) for both sides are applied to delayed nonlinear teleoperation of manipulator robots, and recently, in [35] a position/force control scheme is proposed for bilateral teleoperators with time-varying delays based on the estimation of velocities and forces by using only joint position measurements, assuring that position and force tracking errors become ultimately bounded with arbitrarily small ultimate bound in finite time.

A problem with schemes mentioned is that they must use delayed energy flow or rely heavily on sign functions, adding a discontinuity in control actions as well as controller parameters depending on the environment parameters, making it unfeasible for its application in practice.

Due to the aspects described above, we highlight the need for new control aimed to improve the current overall performance of DBTS in the sense of stability and transparency, via a control scheme applicable in practice. This paper proposes a strategy to get stable coordination for DBTS. The result achieved involves the coordination of force and position. To the best of the authors knowledge, this proposal is novel in the following respects: (a) design of a stable controller for force and motion coordination in a DBTS of a manipulator robot, based on the injection of variable linear damping on the haptic device, avoiding nonlinear damping and discontinuities, thus allowing it to be applied in most commercial robots that include internal configurable PID controllers; (b) the linear damping injected on the local site is changed online based on the time delay and feedback power signal, the latter is defined as the product between leader velocity and delayed environment force, and it is computed only on one side of the delayed teleoperation system allowing to detect immediately when the feedback power injects more energy into the system; (c) simulations using a PELICAN robot and simple experiments are performed evaluating the position and force errors, to verify that such errors hold bounded achieving a simultaneous coordination of force and position.

The paper is presented as follows: Sect. 2 describes the dynamic models, properties, and assumptions used in this work. In Sect. 3, a novel control scheme is proposed, and the stability analysis is performed. Section 5 shows simulation results comparing the proposed scheme with a representative controller of the state of the art, as well as simple experiments applying the scheme proposed. Finally, Sect. 6 shows the discussions and conclusions of the performed simulations and experiments.

1.1 Nomenclature

Table 1 presents the nomenclature used in the mathematical development of this paper.

2 System modeling

To analyze the delayed teleoperation system of a manipulator with force feedback, we first briefly describe the assumptions, properties, and models that this work uses.

Table 1 Nomenclature

Scalars	
K_m, α_m	P+d Parameters of the leader
Δ	Variable linear damping
k_g	Position scaling
k_f	Force scaling
k_s, α_s	P+d Parameters of the follower
k_e, α_e	Parameters of the environment model
g_h, α_h, k_h	Parameters of the human operator model
$h_1, \bar{h_1}$	Forward instantaneous delay and its maximum value
$h_2, \bar{h_2}$	Backward instantaneous delay and its maximum value
E_f	Feedback energy
E_{pd}	Energy of the P+d controller
E_h	Energy of the human operator
E_m	Energy of the haptic device
Vectors ($\mathbb{R}^n$)	
$\mathbf{x}_m, \dot{\mathbf{x}}_m, \ddot{\mathbf{x}}_m$	Position, velocity and acceleration of the leader
$\mathbf{x}_s, \dot{\mathbf{x}}_s, \ddot{\mathbf{x}}_s$	Position, velocity and acceleration of the follower
$\mathbf{f}_h$	Force of the human operator
$\mathbf{f}_e$	Environment force
$\mathbf{g}_m, \mathbf{g}_s$	Gravity forces applied to the leader and follower
$\mathbf{f}_m, \mathbf{f}_s$	Controller output applied to the leader and follower
$\bar{\mathbf{x}}_m, \bar{\mathbf{x}}_s$	Positions of the leader and follower in stationary state
$\bar{\mathbf{f}}_h, \bar{\mathbf{f}}_e$	Forces of the human and environment in stationary state
Matrices ($\mathbb{R}^{n\times n}$)	
$\mathbf{M}_m, \mathbf{M}_s$	Inertia of the leader and follower
$\mathbf{C}_m, \mathbf{C}_s$	Centripetal and Coriolis terms of the leader and follower

2.1 Models

The traditional dynamic model for robot manipulators represented in Cartesian coordinates is used,

$$\mathbf{M}_m(\mathbf{x}_m)\ddot{\mathbf{x}}_\mathbf{m} + \mathbf{C}_m(\mathbf{x}_m, \dot{\mathbf{x}}_\mathbf{m})\dot{\mathbf{x}}_\mathbf{m} + \mathbf{g}_m(\mathbf{x}_m) = \mathbf{f}_m + \mathbf{f}_h, \quad (1)$$

$$\mathbf{M}_s(\mathbf{x}_s)\ddot{\mathbf{x}}_\mathbf{s} + \mathbf{C}_s(\mathbf{x}_s, \dot{\mathbf{x}}_\mathbf{s})\dot{\mathbf{x}}_\mathbf{s} + \mathbf{g}_s(\mathbf{x}_s) = \mathbf{f}_s + \mathbf{f}_e. \quad (2)$$

where $\mathbf{x}_m, \mathbf{x}_s \in R^n$ are the leader and follower positions in Cartesian coordinates, respectively; $\dot{\mathbf{x}}_\mathbf{m}, \dot{\mathbf{x}}_\mathbf{s}$ are the corresponding velocities, $\mathbf{M}_m(\mathbf{x}_m), \mathbf{M}_s(\mathbf{x}_s) \in R^{nxn}$ are the inertia matrices, $\mathbf{C}_m(\mathbf{x}_m, \dot{\mathbf{x}}_\mathbf{m}), \mathbf{C}_s(\mathbf{x}_s, \dot{\mathbf{x}}_\mathbf{s})$ represent the centripetal and Coriolis forces, $\mathbf{g}_m(\mathbf{x}_m), \mathbf{g}_s(\mathbf{x}_s)$ describe the gravitational forces, $\mathbf{f}_h$ and $\mathbf{f}_e$ are the human and environment forces, and $\mathbf{f}_m, \mathbf{f}_s$ represent the forces, computed by the controller. We assume that the robots do not operate in workspace singular points.

2.2 Assumptions and properties

In this work, the following assumptions, properties and lemmas are used [14, 15, 36]:

Property 1 *The inertia matrices* $\mathbf{M_m}$ *and* $\mathbf{M_s}$ *are symmetric positive definite.*

Property 2 *The matrices* $\dot{\mathbf{M}}_\mathbf{m} - 2\mathbf{C}_m$ *and* $\dot{\mathbf{M}}_\mathbf{s} - 2\mathbf{C}_s$ *are skew-symmetric.*

Property 3 *There exist* $\psi_1, \psi_2 > 0$ *such that* $\mathbf{C}_m\dot{\mathbf{x}}_\mathbf{m} \leq \psi_1 |\dot{\mathbf{x}}_\mathbf{m}|$ *and* $\mathbf{C}_s\dot{\mathbf{x}}_\mathbf{s} \leq \psi_2 |\dot{\mathbf{x}}_\mathbf{s}|$ *for all time t.*

Property 4 *If* $\dot{\mathbf{x}}_\mathbf{m}, \ddot{\mathbf{x}}_\mathbf{m}, \dot{\mathbf{x}}_\mathbf{s}, \ddot{\mathbf{x}}_\mathbf{s}$ *are bounded, then the time derivative of* $\mathbf{C}_m$ *and* $\mathbf{C}_s$ *are bounded too.*

Assumption 1 Based on [37]. The communication channel adds forward h_1 and backward h_2 time delays. These delays are time-varying, bounded and asymmetric. Therefore, it is possible to establish $\bar{h}_1$ and $\bar{h}_2$ such that $0 \leq h_1(t) \leq \bar{h}_1$ and $0 \leq h_2(t) \leq \bar{h}_2$ for all t and $\dot{h}_1 < \tau < 1, \dot{h}_2 < \tau < 1$.

Assumption 2 Based on [23]. The remote environment is considered as a viscous-elastic force plus a constant force and a non-modeled signal of finite energy. Such force output is represented by:

$$\mathbf{f}_e = \mathbf{f}_{a_e} - k_e(\mathbf{x}_s - \mathbf{x}_e) - \alpha_e\dot{\mathbf{x}}_\mathbf{s} - \mathbf{B}, \quad (3)$$

where k_e, α_e are the elasticity and damping coefficients of the environment model, the vector $\mathbf{x}_s - \mathbf{x}_e$ represents the distance that penetrates the robot on the elastic medium taking for simplicity $\mathbf{x}_e = \mathbf{0}$, $\mathbf{B}$ is a constant value and $\mathbf{f}_{a_e} \in \mathcal{L}_2 \cap \mathcal{L}_\infty$ represents a bounded-energy non-modeled signal with $\|\mathbf{f}_{a_e}\| \leq \bar{f}_{a_e}$ and $\|\dot{\mathbf{f}}_{a_e}\|$ bounded too, being $\bar{f}_{a_e}$ a positive constant.

Assumption 3 Based on [37], the human operator behaves as a P+d like controller plus and a non-modeled signal of finite energy. Such model is described as follows:

$$\mathbf{f}_h = \mathbf{f}_{a_h} + g_h(\mathbf{A} - \mathbf{x}_s(t - h_2)) - \alpha_h\dot{\mathbf{x}}_\mathbf{m} - k_h\mathbf{x}_\mathbf{m}, \quad (4)$$

where constants $\alpha_h > 0$ and $k_h >$ represent the human operator damping and the elastic coefficient. On the other hand, the mental reference of the operator is assumed to be composed of a constant setpoint A plus a variable part $\mathbf{f}_{a_h} \in \mathcal{L}_2 \cap \mathcal{L}_\infty$ which is assumed to hold $\|\mathbf{f}_{a_h}\| \leq \bar{f}_{a_h}$ and $\|\dot{\mathbf{f}}_{a_h}\|$ bounded, where $\bar{f}_{a_h}$ is a positive constant value. In this sense, g_h is the internal gain of the human operator that is translated into the intensity by which the setpoint is pursued. From a control perspective, A represents the system convergence point in the steady state. Although most models present in the literature are passive [24], this assumption does not cover most of the

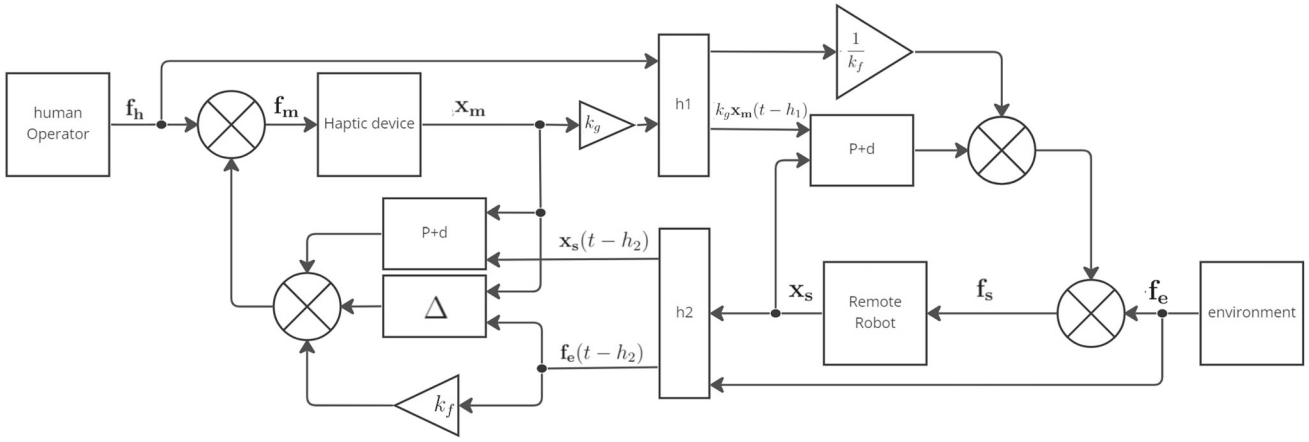

Fig. 1 Control system architecture

tasks that the human operator can perform, which must be explicitly evaluated for each particular task, where the human parameters can be identified following a procedure like [21].

Lemma 1 (Barbalat) [38]. *For any* $\mathbf{f} : R_{\geq 0} \rightarrow R^n$, *if* $\lim_{t\to\infty} \int_0^t \mathbf{f}(\tau)\,\mathrm{d}\tau$ *exists and is finite, and* $\mathbf{f}(t)$ *is uniformly continuous, i.e.,* $\dot{\mathbf{f}}(t) \in \mathcal{L}_\infty$, *then* $\lim_{t\to\infty} \mathbf{f}(t) = 0$. *Besides, for any* $\mathbf{f} : R_{\geq 0} \rightarrow R^n$, *if* $\mathbf{f}(t) \in \mathcal{L}_2 \cap \mathcal{L}_\infty$ *and* $\dot{\mathbf{f}}(t) \in \mathcal{L}_\infty$, *then* $\lim_{t\to\infty} \mathbf{f}(t) = 0$.

Lemma 2 [39] *For vector functions* $\mathbf{a}(.)$, $\mathbf{b}(.)$ *and a variable value* $h(t)$ *with* $0 \leq h(t) \leq \bar{h}$, *the following expression is valid:*

$$-2\mathbf{a}^{\mathsf{T}}(t)\int_{t-h(t)}^{t}\mathbf{b}(\xi)\,\mathrm{d}\xi - \int_{t-h(t)}^{t}\mathbf{b}^{\mathsf{T}}(\xi)\mathbf{b}(\xi)\,\mathrm{d}\xi \leq h(t)\mathbf{a}^{\mathsf{T}}(t)\mathbf{a}(t) \leq \bar{h}(t)\mathbf{a}^{\mathsf{T}}(t)\mathbf{a}(t). \tag{5}$$

3 Controller for force and position coordination

We propose to couple a P+d+f structure (including the interchange of force and position signals between the local and remote sites) with a variable damping depending on a feedback power signal. The controller output $\mathbf{f}_\mathrm{m}$ (applied to the leader) and $\mathbf{f}_\mathrm{s}$ (executed by the follower) is proposed as:

$$\mathbf{f}_\mathrm{m} = -k_\mathrm{m}(k_\mathrm{g}\mathbf{x}_\mathrm{m} - \mathbf{x}_\mathrm{s}(t-h_2)) - (\alpha_\mathrm{m}+\Delta)\dot{\mathbf{x}}_\mathbf{m} + \mathbf{g}_\mathrm{m}(\mathbf{x}_\mathrm{m}) + k_\mathrm{f}\mathbf{f}_\mathrm{e}(t-h_2), \tag{6}$$

$$\mathbf{f}_\mathrm{s} = k_\mathrm{s}(k_\mathrm{g}\mathbf{x}_\mathrm{m}(t-h_1) - \mathbf{x}_\mathrm{s}) - \alpha_\mathrm{s}\dot{\mathbf{x}}_\mathbf{s} + \mathbf{g}_\mathrm{s}(\mathbf{x}_\mathrm{s}) + \frac{1}{k_\mathrm{f}}\mathbf{f}_\mathrm{h}(t-h_1), \tag{7}$$

where the parameters k_s and k_m represent gain values, k_g maps the haptic device position to the remote robot set point, k_f describes a force scaling, α_m and α_s are damping coefficients, and Δ represents a variable linear damping that will depend on the feedback power signal measurable on the local site.

This scheme is compatible with the internal structure of commercial manipulator robots which commonly are based on PID (or modified PID) controllers. Figure 1 presents the architecture of the control system.

To understand how the proposal works, we analyze the energies involved in the leader. First, we define the feedback power signal P_{df} as the product of the leader velocity and the delayed environment force (8). This signal will be used in Δ to vary the total damping of the leader, and in doing so, indirectly control the total energy

$$P_{df} = k_\mathrm{f}\dot{\mathbf{x}}_\mathbf{m}^T(\varepsilon)\,\mathbf{f_e}(\varepsilon - h_2). \tag{8}$$

The energy E_Pd (10) is the result of the force $\mathbf{f_{ctr}}$ (9) applied by the P+d (Proportional plus damping) controller used in the haptic device (6)

$$\mathbf{f_{ctr}} = -k_\mathrm{m}(k_\mathrm{g}\mathbf{x}_\mathrm{m} - \mathbf{x}_\mathrm{s}(t-h_2)) - (\alpha_\mathrm{m}+\Delta)\dot{\mathbf{x}}_\mathbf{m} + \mathbf{g}_\mathrm{m}(\mathbf{x}_\mathrm{m}), \tag{9}$$

$$E_\mathrm{Pd} = \int_0^t \dot{\mathbf{x}}_\mathbf{m}^T(\varepsilon)\,\mathbf{f_{ctr}}(\varepsilon)\,\mathrm{d}\varepsilon. \tag{10}$$

The human operator energy E_h is the result of the force that the operator applies to the haptic device (11)

$$E_\mathrm{h} = \int_0^t \dot{\mathbf{x}}_\mathbf{m}^T(\varepsilon)\,\mathbf{f_h}(\varepsilon)\,\mathrm{d}\varepsilon. \tag{11}$$

When the force of the remote environment (with its corresponding transmission delay) is applied to the haptic device, a new energetic component is introduced in the haptic device that we call feedback energy E_f (12)

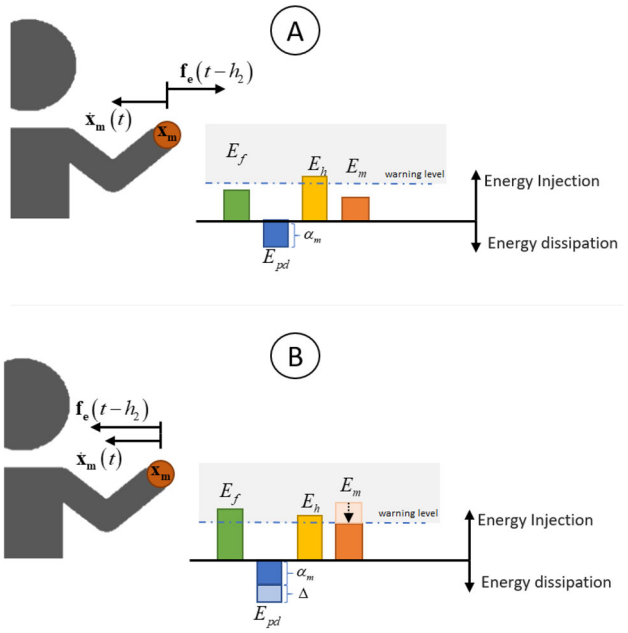

Fig. 2 Given an arbitrary defined energy warning level; Case **A**) When feedback energy (E_f) is outside this level, energy injection mainly occurs by E_h due to time delay; in this situation P+d controller dissipates energy through constant damping. Case **B**) When $\dot{\mathbf{x}}_\mathbf{m}$ points in same direction as $\mathbf{f}_\mathrm{e}(t-h_2)$, E_f increases, then variable damping Δ is used to dissipate the additional energy

$$E_\mathrm{f} = \int_0^t k_\mathrm{f} \dot{\mathbf{x}}_\mathbf{m}^T(\varepsilon)\, \mathbf{f}_\mathbf{e}(\varepsilon - h_2)\, \mathrm{d}\varepsilon. \tag{12}$$

Finally, the haptic device energy E_m is computed as the sum of E_Pd, E_h and E_f (13)

$$E_\mathrm{m} = E_\mathrm{Pd} + E_\mathrm{f} + E_\mathrm{h}. \tag{13}$$

According to the state of the art, the added constant linear damping depends mainly on time delays. We join this concept with variable damping, obtaining a novel $\mathbf{f_{ctr}}$ that reduces the kinetic energy to the extent that the feedback power injects more energy into the system. In contrast, when the feedback power draws energy from the leader, the proposed controller raises the damping only as a function of the time delay. This concept is illustrated in Fig. 2.

3.1 Stability analysis

First, case $\mathbf{A} = \mathbf{B} = \mathbf{0}$ in (3) and (4) will be analyzed. The control error is defined as $\mathbf{e} = k_\mathrm{g}\mathbf{x}_\mathrm{m} - \mathbf{x}_\mathrm{s}$. A positive definite functional $V(\mathbf{x}_\mathrm{m}, \dot{\mathbf{x}}_\mathbf{m}, k_\mathrm{g}\mathbf{x}_\mathrm{m} - \mathbf{x}_\mathrm{s}, \mathbf{x}_\mathrm{s}, \dot{\mathbf{x}}_\mathbf{s}) = V_1 + V_2 + V_3 + V_4$ is proposed and how its time evolution is, along the trajectories of the system from a finite initial condition. The functional is formed by the following terms:

$$V_1 = \frac{1}{2}\dot{\mathbf{x}}_\mathbf{m}^\mathsf{T}\mathbf{M}_\mathrm{m}(\mathbf{x}_\mathrm{m})\dot{\mathbf{x}}_\mathbf{m} + \frac{1}{2}\kappa_1 {\mathbf{x}_\mathrm{m}}^\mathsf{T}\mathbf{x}_\mathrm{m}, \tag{14}$$

$$V_2 = \frac{\kappa_2}{2}\mathbf{e}^\mathsf{T}\mathbf{e}, \tag{15}$$

$$V_3 = \frac{\kappa_3}{2}{\mathbf{x}_\mathrm{s}}^\mathsf{T}\mathbf{x}_\mathrm{s} + \frac{\kappa_4}{2}\dot{\mathbf{x}}_\mathbf{s}^\mathsf{T}\mathbf{M}_\mathrm{s}(\mathbf{x}_\mathrm{s})\dot{\mathbf{x}}_\mathbf{s}, \tag{16}$$

$$\begin{aligned} V_4 = &\int_{-h_2}^{0}\int_{t+\theta}^{t} \dot{\mathbf{x}}_\mathbf{s}^\mathsf{T}(\xi)\dot{\mathbf{x}}_\mathbf{s}(\xi)\,\mathrm{d}\xi\,\mathrm{d}\theta \\ &+ \kappa_4\int_{-h_1}^{0}\int_{t+\theta}^{t} \dot{\mathbf{x}}_\mathbf{m}^\mathsf{T}(\xi)\dot{\mathbf{x}}_\mathbf{m}(\xi)\,\mathrm{d}\xi\,\mathrm{d}\theta \\ &+ \kappa_4\int_{-h_1-h_2}^{0}\int_{t+\theta}^{t} \dot{\mathbf{x}}_\mathbf{s}^\mathsf{T}(\xi)\dot{\mathbf{x}}_\mathbf{s}(\xi)\,\mathrm{d}\xi\,\mathrm{d}\theta \\ &+ \frac{1}{4}\frac{\kappa_4\alpha_\mathrm{h}}{1-\tau}\int_{t-h_1}^{t} \dot{\mathbf{x}}_\mathbf{m}^\mathsf{T}(\xi)\dot{\mathbf{x}}_\mathbf{m}(\xi)\,\mathrm{d}\xi. \end{aligned} \tag{17}$$

Here, $\kappa_i \in \mathbb{R}^+$ are positive constants defined in "Appendix A".

Going on the procedure given in "Appendix A", $\dot{V}$ along the trajectories of the system is analyzed considering the closed-loop dynamics of both leader and follower, time delay, and the human operator and environment forces. As a result, we get:

$$\begin{aligned} \dot{V} \le &-(\lambda_\mathrm{m} + \Delta)\dot{\mathbf{x}}_\mathbf{m}^\mathsf{T}\dot{\mathbf{x}}_\mathbf{m} - \lambda_\mathrm{s}\kappa_4\dot{\mathbf{x}}_\mathbf{s}^\mathsf{T}\dot{\mathbf{x}}_\mathbf{s} \\ &+\rho_\mathrm{m}\,|\dot{\mathbf{x}}_\mathbf{m}| + \rho_\mathrm{s}\,|\dot{\mathbf{x}}_\mathbf{s}| + k_\mathrm{f}\dot{\mathbf{x}}_\mathbf{m}^\mathsf{T}\mathbf{f}_\mathrm{e}(t-h_2), \end{aligned} \tag{18}$$

where

$$\begin{aligned} \lambda_\mathrm{m} &= \alpha_\mathrm{m} + \left(1 - \tfrac{\kappa_4}{4(1-\tau)}\right)\alpha_\mathrm{h} - \kappa_4\bar{h}_1 - \tfrac{1}{4}(k_\mathrm{m} - g_\mathrm{h})^2\bar{h}_2, \\ \lambda_\mathrm{s} &= \alpha_\mathrm{s} + \alpha_\mathrm{e} - \left(1 + \left(\tfrac{k_\mathrm{s}k_\mathrm{g}}{2}\right)^2 + \left(\tfrac{g_\mathrm{h}}{2k_\mathrm{f}}\right)^2\right) \\ &\quad \bar{h}_1 - \left(1 + \tfrac{1}{\kappa_4} + \left(\tfrac{g_\mathrm{h}}{2k_\mathrm{f}}\right)^2\right)\bar{h}_2, \end{aligned} \tag{19}$$

$$\begin{aligned} \rho_\mathrm{m} &= \mathbf{f}_{\mathrm{a_h}}, \\ \rho_\mathrm{s} &= \kappa_4\left(\tfrac{1}{k_\mathrm{f}}\mathbf{f}_{\mathrm{a_h}}(t-h_1) - \mathbf{f}_{\mathrm{a_e}}\right), \end{aligned} \tag{20}$$

with $\kappa_4 := (k_\mathrm{m} - g_\mathrm{h})/(k_\mathrm{s}k_\mathrm{g})$.

From (18) to achieve bounded velocities, we design Δ to dynamically compensate the term $x = k_\mathrm{f}\dot{\mathbf{x}}_\mathbf{m}^\mathsf{T}\mathbf{f}_\mathrm{e}(t-h_2)$, called feedback power signal, measurable on the local site.

We propose Δ to comply with the following general conditions:

1. $\Delta(x)$ varies with the feedback power, i.e., $\Delta(x) = f(\dot{\mathbf{x}}_\mathbf{m}^\mathsf{T}\mathbf{f}_\mathrm{e}(t-h_2))$.
2. $\Delta(x)$ only extracts energy from system, then $\Delta(x) \ge 0 \forall x$.

3. To preserve transparency, $\Delta(x)$ must remain low when the direction of $\dot{\mathbf{x}}_\mathbf{m}$ and $\mathbf{f}_\mathrm{e}(t-h_2)$ are opposite, i.e., $\lim_{x\to-\infty}\Delta(x)=0$.
4. When the direction of $\dot{\mathbf{x}}_\mathbf{m}$ and $\mathbf{f}_\mathrm{e}(t-h_2)$ are the same, $\Delta(x)$ must be a monotonically increasing function with respect to the feedback power, i.e., if $x\le y$ then $\Delta(x)\le\Delta(y)$.
5. To preserve the stability of the system when the direction of $\dot{\mathbf{x}}_\mathbf{m}$ and $\mathbf{f}_\mathrm{e}(t-h_2)$ are the same, the power extracted by $\Delta(x)$ must be greater than the power of the feedback signal, i.e., $\dot{\mathbf{x}}_\mathbf{m}^\mathsf{T}\Delta\dot{\mathbf{x}}_\mathbf{m}\ge k_\mathrm{f}\dot{\mathbf{x}}_\mathbf{m}^\mathsf{T}\mathbf{f}_\mathrm{e}(t-h_2)\forall\dot{\mathbf{x}}_\mathbf{m}^\mathsf{T}\mathbf{f}_\mathrm{e}(t-h_2)>0$.

Remark 1 If α_m and α_s are sufficiently big (high damping) to fulfill $\lambda_\mathrm{m},\lambda_\mathrm{s}>0$ (19), the condition $k_\mathrm{m}>g_\mathrm{h}$ is hold, then we can get from V (14)–(17) and $\dot{V}$ (18) that variables $\dot{\mathbf{x}}_\mathbf{m}$, $\dot{\mathbf{x}}_\mathbf{s}\in\mathcal{L}_\infty$.

Next, if (18) is integrated with respect to time, we get:

$$V(t)-V(0)\le-\lambda_\mathrm{m}\|\dot{\mathbf{x}}_\mathbf{m}\|_2^2-\lambda_\mathrm{s}\|\dot{\mathbf{x}}_\mathbf{s}\|_2^2+\int_0^t\dot{\mathbf{x}}_\mathbf{m}^\mathsf{T}(\varepsilon)\rho_\mathrm{m}(\varepsilon)\,\mathrm{d}\varepsilon+\int_0^t\dot{\mathbf{x}}_\mathbf{s}^\mathsf{T}(\varepsilon)\rho_\mathrm{s}(\varepsilon)\,\mathrm{d}\varepsilon+\int_0^t\dot{\mathbf{x}}_\mathbf{m}^\mathsf{T}(-\Delta(\varepsilon)\dot{\mathbf{x}}_\mathbf{m}+k_\mathrm{f}\mathbf{f}_\mathrm{e}(\varepsilon-h_2))\,\mathrm{d}\varepsilon. \tag{21}$$

Remark 2 The integral terms $\int_0^t\dot{\mathbf{x}}_\mathbf{m}(\varepsilon)^\mathsf{T}\rho_\mathrm{m}(\varepsilon)\,\mathrm{d}\varepsilon$ and $\int_0^t\dot{\mathbf{x}}_\mathbf{s}(\varepsilon)^\mathsf{T}\rho_\mathrm{s}2(\varepsilon)\,\mathrm{d}\varepsilon$ are bounded since $\mathbf{f}_{\mathrm{a}_\mathrm{e}},\mathbf{f}_{\mathrm{a}_\mathrm{h}}\in\mathcal{L}_2$ (Assumptions 2 and 3) and $\dot{\mathbf{x}}_\mathbf{m},\dot{\mathbf{x}}_\mathbf{s}\in\mathcal{L}_\infty$.

The design of the variable damping Δ allows that

$$\int_0^t\dot{\mathbf{x}}_\mathbf{m}^\mathsf{T}(-\Delta(\varepsilon)\dot{\mathbf{x}}_\mathbf{m}+k_\mathrm{f}\mathbf{f}_\mathrm{e}(\varepsilon-h_2))\,\mathrm{d}\varepsilon\le0,$$

and due to V is radially unbounded, we get V bounded in (21) for all t, hence $\mathbf{x}_\mathrm{m},\mathbf{x}_\mathrm{s}\in\mathcal{L}_\infty$. Therefore, $\|\dot{\mathbf{x}}_\mathbf{m}\|_2^2$ and $\|\dot{\mathbf{x}}_\mathbf{s}\|_2^2$ are bounded too, which implies that $\dot{\mathbf{x}}_\mathbf{m},\dot{\mathbf{x}}_\mathbf{s}\in\mathcal{L}_2$. It is important to remark that as greater the magnitude of Δ is, the system better avoids the possible increase of the feedback power injected to the leader, while if such control parameter is low, the transparency is higher. Consequently, the selection of Δ must take into account a trade-off between stability (energy boundness) and transparency (the human operator perceiving the environment such as it is). Because of this trade-off, the expression of Δ is a design factor that must be selected for each particular application. Without losing generality, in Sect. 5 we propose a possible expression for Δ.

In addition, the closed-loop dynamics of the leader (1) and follower (2), including the proposed controller in (6) and (7), can be represented by the following expressions:

$$\ddot{\mathbf{x}}_\mathbf{m}=\mathbf{M}_\mathbf{m}^{-1}\Big[-\mathbf{C}_\mathrm{m}\dot{\mathbf{x}}_\mathbf{m}-k_\mathrm{m}(k_\mathrm{g}\mathbf{x}_\mathrm{m}-\mathbf{x}_\mathrm{s}(t-h_2))-(\alpha_\mathrm{m}+\Delta)\dot{\mathbf{x}}_\mathbf{m}+k_\mathrm{f}\mathbf{f}_\mathrm{e}(t-h_2)+\mathbf{f}_\mathrm{h}\Big], \tag{22}$$

$$\ddot{\mathbf{x}}_\mathbf{s}=\mathbf{M}_\mathbf{s}^{-1}\Big[-\mathbf{C}_\mathrm{s}\dot{\mathbf{x}}_\mathbf{s}+k_\mathrm{s}(k_\mathrm{g}\mathbf{x}_\mathrm{m}(t-h_1)-\mathbf{x}_\mathrm{s})-\alpha_\mathrm{s}\dot{\mathbf{x}}_\mathbf{s}+\tfrac{1}{k_\mathrm{f}}\mathbf{f}_\mathrm{h}(t-h_1)+\mathbf{f}_\mathrm{e}\Big]. \tag{23}$$

Remark 3 Due to *Remark* 1 and 2, $\dot{\mathbf{x}}_\mathbf{m},\dot{\mathbf{x}}_\mathbf{s}\in\mathcal{L}_\infty\cap\mathcal{L}_2$, and therefore, $\int_0^t\dot{\mathbf{x}}_\mathbf{m}\,\mathrm{d}t$ and $\int_0^t\dot{\mathbf{x}}_\mathbf{s}\,\mathrm{d}t$ have finite limit for $t\to\infty$. Furthermore, all terms on the right hand of (22) and (23) are bounded from *Remark* 1 and Assumptions 1, 2 and 3; i.e., $\dot{\mathbf{x}}_\mathbf{m},\dot{\mathbf{x}}_\mathbf{s}$ are uniformly continuous. Next, Lemma 1 can be applied concluding that $\dot{\mathbf{x}}_\mathbf{m},\dot{\mathbf{x}}_\mathbf{s}\to\mathbf{0}$ as $t\to\infty$. Lemma 1 can also be applied to $\int_0^t\ddot{\mathbf{x}}_\mathbf{m}(\varepsilon)\,\mathrm{d}\varepsilon$ and $\int_0^t\ddot{\mathbf{x}}_\mathbf{s}(\varepsilon)\,\mathrm{d}\varepsilon$, which have finite and defined limit for $t\to\infty$. Deriving (22) and (23) it is feasible to verify that $\dddot{\mathbf{x}}_\mathbf{m}$ and $\dddot{\mathbf{x}}_\mathbf{s}$ are bounded; then we get as the result that $\ddot{\mathbf{x}}_\mathbf{m},\ddot{\mathbf{x}}_\mathbf{s}\to\mathbf{0}$ as $t\to\infty$. We remark that from this result it is possible to infer that $\Delta(x)\to0$ for $t\to\infty$, which implies that the total damping of the haptic device tends to α_m.

3.2 Force and position dual coordination

To obtain 1, 2 and 3, $\mathbf{A}=\mathbf{B}=\mathbf{0}$ was considered. Otherwise, a variable change is performed in order that a similar stability analysis can be carried out [34].

To get the new Krasovskii-like equilibrium solution the closed-loop dynamics is analyzed for $t\to\infty$, in this situation let us assume that $\dot{\mathbf{x}}_\mathbf{m},\ddot{\mathbf{x}}_\mathbf{m},\dot{\mathbf{x}}_\mathbf{s},\ddot{\mathbf{x}}_\mathbf{s}\to\mathbf{0}$, considering $\mathbf{A}$ and $\mathbf{B}$ as constant values. Next, the following relations in stationary state can be expressed from (22) and (23):

$$-k_\mathrm{m}(k_\mathrm{g}\bar{\mathbf{x}}_\mathbf{m}-\bar{\mathbf{x}}_\mathbf{s})+k_\mathrm{f}\bar{\mathbf{f}}_\mathbf{e}+\bar{\mathbf{f}}_\mathbf{h}=\mathbf{0}, \tag{24}$$

$$k_\mathrm{s}(k_\mathrm{g}\bar{\mathbf{x}}_\mathbf{m}-\bar{\mathbf{x}}_\mathbf{s})+\tfrac{1}{k_\mathrm{f}}\bar{\mathbf{f}}_\mathbf{h}+\bar{\mathbf{f}}_\mathbf{e}=\mathbf{0}, \tag{25}$$

where $\bar{\mathbf{x}}_\mathbf{m}:=\lim_{t\to\infty}\mathbf{x}_\mathrm{m}(t)$, $\bar{\mathbf{x}}_\mathbf{s}:=\lim_{t\to\infty}\mathbf{x}_\mathrm{s}(t)$, $\bar{\mathbf{f}}_\mathbf{h}:=\lim_{t\to\infty}\mathbf{f}_\mathrm{h}(t)$ and $\bar{\mathbf{f}}_\mathbf{e}:=\lim_{t\to\infty}\mathbf{f}_\mathrm{e}(t)$. Observing (24) and (25), it is possible to infer that:

$$\bar{\mathbf{x}}_\mathbf{s}\to k_\mathrm{g}\bar{\mathbf{x}}_\mathbf{m}\quad\text{and}\quad k_\mathrm{f}\bar{\mathbf{f}}_\mathbf{e}\to-\bar{\mathbf{f}}_\mathbf{h}. \tag{26}$$

Next, if the proposed human operator model (4) and the environment force (3) are included into (26), the relations represented below can be achieved at steady state:

$$k_\mathrm{f}\bar{\mathbf{f}}_\mathbf{e}=-k_\mathrm{f}k_\mathrm{e}\bar{\mathbf{x}}_\mathbf{s}-k_\mathrm{f}\mathbf{B}=-\bar{\mathbf{f}}_\mathbf{h}=-g_\mathrm{h}(\mathbf{A}-\bar{\mathbf{x}}_\mathbf{s}),\qquad\bar{\mathbf{x}}_\mathbf{m}\to\frac{(g_\mathrm{h}\mathbf{A}-k_\mathrm{f}\mathbf{B})}{(k_\mathrm{e}k_\mathrm{g}k_\mathrm{f}+g_\mathrm{h}k_\mathrm{g}+k_\mathrm{h})}. \tag{27}$$

Finally, analyzing (26) and (27), the following variable change is proposed:

$$\mathbf{x} = \mathbf{x}_{\mathrm{m}} - \bar{\mathbf{x}}_{\mathbf{m}}, \tag{28}$$

$$\mathbf{y} = \mathbf{x}_{\mathrm{s}} - \bar{\mathbf{x}}_{\mathbf{s}}, \tag{29}$$

where $\bar{\mathbf{x}}_{\mathbf{m}}$ and $\bar{\mathbf{x}}_{\mathbf{s}}$ are constant values. If (28) and (29) are applied to (22) and (23), and on the resulting relations the proposed human operator model (4) and the environment force (3) are included, then it is possible to get the following equations to represent the DBTS:

$$\begin{aligned}\ddot{\mathbf{x}} = \mathbf{M}_{\mathbf{m}}^{-1}\Big[& -\mathbf{C}_{\mathrm{m}}\dot{\mathbf{x}} \\ & - k_{\mathrm{m}}(k_{\mathrm{g}}(\mathbf{x}+\bar{\mathbf{x}}_{\mathbf{m}}) - (\mathbf{y}(t-h_2)+\bar{\mathbf{x}}_{\mathbf{s}})) \\ & - (\alpha_{\mathrm{m}}+\Delta)\dot{\mathbf{x}} \\ & + k_{\mathrm{f}}(\mathbf{f}_{\mathrm{a_e}}(t-h_2) - k_{\mathrm{e}}(\mathbf{y}(t-h_2)+\bar{\mathbf{x}}_{\mathbf{s}}) \\ & - \alpha_{\mathrm{e}}\dot{\mathbf{y}}(t-h_2)+\mathbf{B}) \\ & + \mathbf{f}_{\mathrm{a_h}} + g_{\mathrm{h}}(\mathbf{A} - (\mathbf{y}(t-h_2)+\bar{\mathbf{x}}_{\mathbf{s}})) \\ & - \alpha_{\mathrm{h}}\dot{\mathbf{x}} - k_{\mathrm{h}}(\mathbf{x}+\bar{\mathbf{x}}_{\mathbf{m}})\Big],\end{aligned} \tag{30}$$

$$\begin{aligned}\ddot{\mathbf{y}} = \mathbf{M}_{\mathbf{s}}^{-1}\Big[& -\mathbf{C}_{\mathrm{s}}\dot{\mathbf{y}} + k_{\mathrm{s}}(k_{\mathrm{g}}(\mathbf{x}(t-h_1) \\ & + \bar{\mathbf{x}}_{\mathbf{m}}) - (\mathbf{y}+\bar{\mathbf{x}}_{\mathbf{s}})) - \alpha_{\mathrm{s}}\dot{\mathbf{y}} \\ & + \tfrac{1}{k_{\mathrm{f}}}(\mathbf{f}_{\mathrm{a_h}}(t-h_1) + g_{\mathrm{h}}(\mathbf{A} - (\mathbf{y}(t-h_1-h_2) \\ & + \bar{\mathbf{x}}_{\mathbf{s}})) - \alpha_{\mathrm{h}}\dot{\mathbf{x}}(t-h_1)) \\ & + \mathbf{f}_{\mathrm{a_e}} - k_{\mathrm{e}}(\mathbf{y}+\bar{\mathbf{x}}_{\mathbf{s}}) - \alpha_{\mathrm{e}}\dot{\mathbf{y}} + \mathbf{B} - k_{\mathrm{h}}(\mathbf{x}(t-h_1)+\bar{\mathbf{x}}_{\mathbf{m}})\Big].\end{aligned} \tag{31}$$

Now, if $\hat{\mathbf{f}}_{\mathbf{h}}$ and $\hat{\mathbf{f}}_{\mathbf{e}}$ are defined by:

$$\begin{aligned}\hat{\mathbf{f}}_{\mathbf{h}} &= \mathbf{f}_{\mathrm{a_h}} + g_{\mathrm{h}}\mathbf{y}(t-h_2) - \alpha_{\mathrm{h}}\dot{\mathbf{x}} - k_{\mathrm{h}}\mathbf{x}, \\ \hat{\mathbf{f}}_{\mathbf{e}} &= \mathbf{f}_{\mathrm{a_e}} - k_{\mathrm{e}}\mathbf{y} - \alpha_{\mathrm{e}}\dot{\mathbf{y}}.\end{aligned} \tag{32}$$

Then, considering the relations (26) and (27), equations (30) and (31) can be rewritten, in a similar way to (22) and (23), as follows:

$$\begin{aligned}\ddot{\mathbf{x}} = \mathbf{M}_{\mathbf{m}}^{-1}\Big[& -\mathbf{C}_{\mathrm{m}}\dot{\mathbf{x}} - k_{\mathrm{m}}(k_{\mathrm{g}}\mathbf{x} \\ & - \mathbf{y}(t-h_2)) - (\alpha_{\mathrm{m}}+\Delta)\dot{\mathbf{x}} + k_{\mathrm{f}}\hat{\mathbf{f}}_{\mathbf{e}}(t-h_2) \\ & + \hat{\mathbf{f}}_{\mathbf{h}}\Big],\end{aligned} \tag{33}$$

$$\begin{aligned}\ddot{\mathbf{y}} = \mathbf{M}_{\mathbf{s}}^{-1}\Big[& -\mathbf{C}_{\mathrm{s}}\dot{\mathbf{y}} + k_{\mathrm{s}}(k_{\mathrm{g}}\mathbf{x}(t-h_1) - \mathbf{y}) \\ & - \alpha_{\mathrm{s}}\dot{\mathbf{y}} + \tfrac{1}{k_{\mathrm{f}}}\hat{\mathbf{f}}_{\mathbf{h}}(t-h_1) + \hat{\mathbf{f}}_{\mathbf{e}}\Big].\end{aligned} \tag{34}$$

Remark 4 A procedure similar to the one carried on *Remark* 1, 2 and 3 can be applied to the delayed system represented by (33) and (34), getting as a result that the teleoperation system converges for $t \to \infty$ to an equilibrium in which a simultaneous synchronism of force (force exerted by the human operator will tend to the scaled environment force) and motion (the position mapped linearly by the leader will tend to the follower's position) is obtained. Besides, the human operator can change the convergence point handling their internal reference $\mathbf{A}$.

4 Experimental results

In this section, the system is implemented in practice. In these experiments, a human operator commands a remote manipulator robot through a network, to execute an inspection by contact of a soft medium. Novint Falcon is used as a 3D haptic joystick to drive a Robotis Manipulator-H as the remote robot. The human and the environment forces are measured with a Variense 3-axis force sensor, model fs103. Each device runs in a separate computer and is linked with a Ubiquiti NanoStation long-range antenna. Each device (sensors and robots) is controlled employing independent executable programs developed in C++ language. Moreover, the controllers are implemented within Matlab Simulink running in real-time mode. All internal software modules of each computer communicate with each other through shared memory. A layout of the experimental setup and views of the local and remote sites is shown in Figs. 3 and 4, respectively.

The performed test involves utilizing a remotely teleoperated manipulator, controlled over the network, to conduct a horizontal scan on a soft surface while maintaining a nearly constant vertical force. The human operator's task is to position the robot in contact with the medium and assess its hardness by exerting a displacement/force along the z-axis. Subsequently, the operator must examine the medium's resistance to movement by applying a displacement/force along the y-axis while keeping the z-axis position and force as constant as possible. Finally, the operator is required to return the robot to its initial position.

Although the desired position command A is not explicitly given to the operator, maintaining a constant contact force with a passive medium implies A to be constant and $B = 0[N]$. The medium is positioned at the origin of the z-axis.

A video demonstrating teleoperation with high delay can be viewed here.

Experiments are repeated for three different communication time delays $h = h_1 + h_2$: low, medium, and high.

For medium and high delay, a simulated time-variant delay is added to both incoming and outcoming signals. These delays h_i are generated by random sinusoidal signals mounted on random constant with the addition of white noise. The linear damping is qualitatively calibrated for each test based on (19).

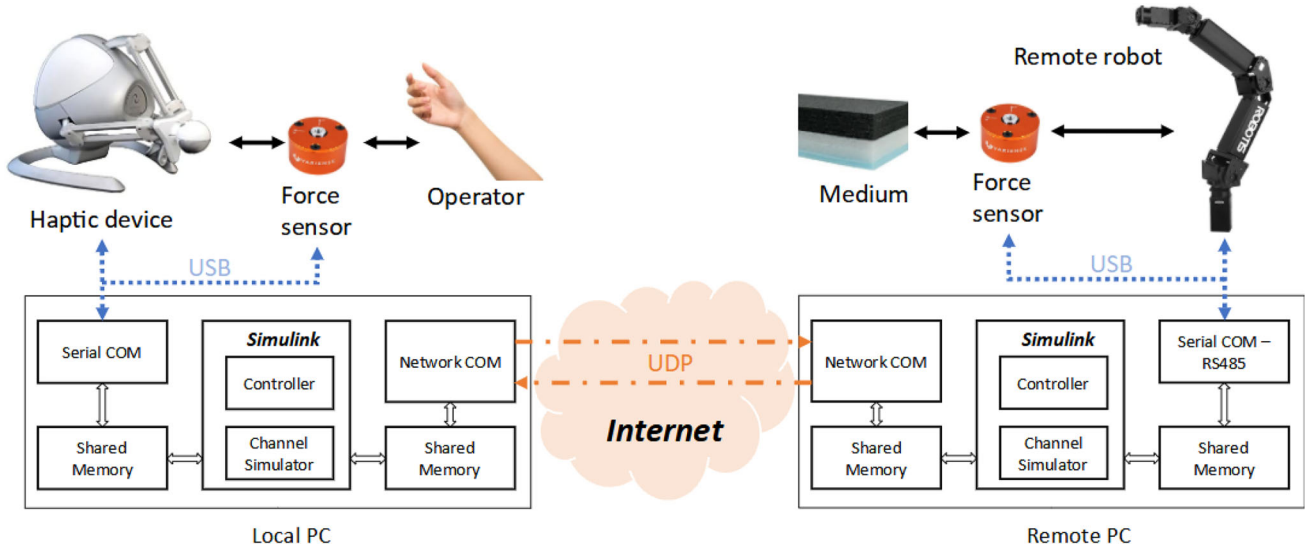

Fig. 3 Experimental setup

Fig. 4 Views of the remote site (bigger picture) and local site (bottom-right picture)

4.1 Setup

For the controller implementation, first an expression for $\Delta(t)$ is chosen, following the guidelines of Sect. 3.1. For a sake of simplicity we propose to use the function:

$$\Delta = k_{\alpha 1} e^{k_{\alpha 2} \dot{\mathbf{x}}_{\mathbf{m}}^{\mathrm{T}} \mathbf{f}_{\mathrm{e}} (t - h_2)}, \tag{35}$$

where $k_{\alpha i}$ are positive constants, which was adjusted empirically: first performing an experiment and measuring the maximum value of the feedback power, then choosing a value high enough to ensure the condition 3.1. The parameters used in each experiment are summarized in Table 2.

Table 2 Parameters used in the experiments

Parameter	Low delay	Medium delay	High delay
$\max(h)$ [s]	0.5	1.5	2.25
k_{m} [kg/s^2]	8	8	8
k_{s} [kg/s^2]	10	10	10
k_{g} [m/m]	1	1	1
k_{f} [N/N]	1	1	1
$k_{\alpha 1}$ [kg/s]	0.2	0.4	0.6
$k_{\alpha 2}$ [s^3/ (kg $\cdot$ m^2)]	20	20	20
g_{h} [kg/s^2]	5	5	5
α_{h} [kg/s]	0.5	0.5	0.5
α_{e} [kg/s]	0.5	0.5	0.5
τ [N]	0.5	0.5	0.5

On the other hand, α_{m} and α_{s} values were calculated for each h_i using (19).

4.2 Results

Figures 5, 6 and 7 show the results of the experiments. Despite the time delay (last graph in each figure), accurate position tracking on both the y-axis and z-axis is observed. In addition, even when the forces signals are (as usual) very noisy, a good force tracking of the system is observed in both, waveform and magnitude. It should be noted that the force synchronization occurs only when the robot is in contact with the medium, that is, $F_{\mathrm{e}} \neq 0[N]$. When $F_{\mathrm{e}} = 0[N]$ the force desynchronism occurs because the operator pushes the end

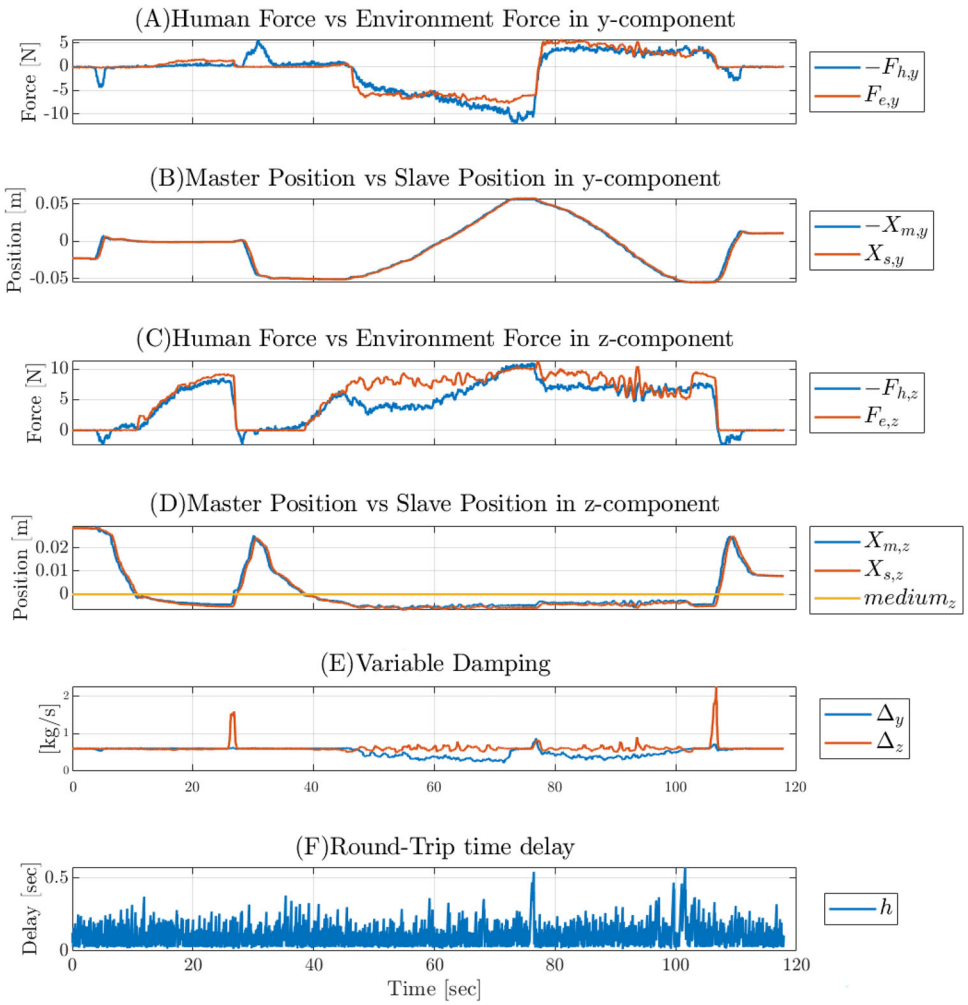

Fig. 5 Experimental results for low delay. **A** Environment-operator force tracking on the y-axis. **B** Environment-operator position tracking on the y-axis. **C** Environment-operator force tracking on the z-axis. **D** Environment-operator position tracking on the z-axis and position of the medium. **E** Evolution of variable damping. **F** Round-trip communication delay

effector of the haptic device, and therefore generates a measurement in the sensor.

Next, tracking error index of position $\mathrm{I_x}$ and force $\mathrm{I_f}$ and time to complete the task $\mathrm{T_{task}}$ are obtained. Such metrics are calculated as follows:

$$\mathrm{I_x} = \frac{1}{\mathrm{T_{task}}} \int_0^{\mathrm{T_{task}}} |\mathbf{x}_\mathrm{m}(\xi) - \mathbf{x}_\mathrm{s}(\xi)| \, \mathrm{d}\xi, \tag{36}$$

$$\mathrm{I_f} = \frac{1}{\mathrm{T_{task}}} \int_0^{\mathrm{T_{task}}} |\mathbf{f}_\mathrm{h}(\xi) - \mathbf{f}_\mathrm{e}(\xi)| \, \mathrm{d}\xi. \tag{37}$$

Remark are summarized in Table 3.

From Table 3 and Figs. 5, 6 and 7, it can be seen that, as usual, system performance degrades as the time delay grows. However, it is observed that even under a high time delay of more than 2 s, the system behaves adequately, keeping the main control variables bounded, which translates into satisfactory performance in terms of stability and transparency.

5 Simulations

In this section, simulation results are presented to compare general aspects of the response of the proposed scheme with the one obtained using the controller from [34], since the latter is a good representative of the controllers were the stability condition is reached through control actions with sign functions.

Some key differences and similarities of our proposal with the most well-known papers of the state of the art are summarized in Table 4. It is important to note that our proposal doesn't require the use of sign functions or the cancellation of exogenous forces. Its parameters are independent of the elasticity of the medium and it modifies the damping depending on a measurable power/energy signal; this way it avoids the use of observers whose estimation usually degrades with the time delay.

To contrast the results, the response of the system is compared with the case without variable damping. It should be noted that there is no theoretical evidence of the stability of

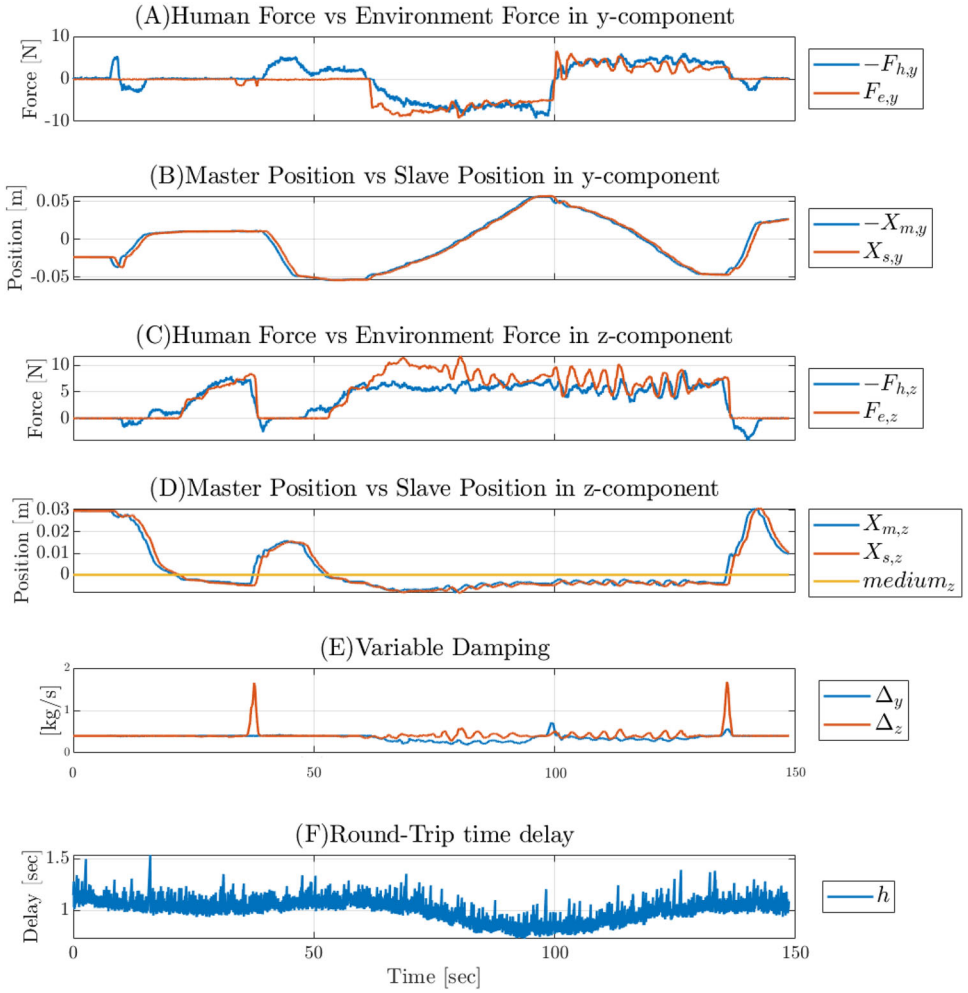

Fig. 6 Experimental results for medium delay. **A** Environment-operator force tracking on the y-axis. **B** Environment-operator position tracking on the y-axis. **C** Environment-operator force tracking on the z-axis. **D** Environment-operator position tracking on the z-axis and position of the medium. **E** Evolution of variable damping. **F** Round-trip communication delay

the latter, despite the fact that it performs well in these few simulations.

The controllers are constructed from Eqs. (6) and (7). In the first controller (denoted as $Pdf+\Delta$), Δ is chosen following the guidelines of Sect. 3.1. For the sake of simplicity, we propose to use the following function

$$\Delta = k_{\alpha 1} e^{k_{\alpha 2} \dot{\mathbf{x}}_{\mathbf{m}}^{\mathsf{T}} \mathbf{f}_{\mathrm{e}}(t-h_2)}, \tag{38}$$

where $k_{\alpha i}$ are positive constants, which were adjusted empirically: first performing a simulation and measuring the maximum value of the feedback power, then choosing a value high enough to ensure the condition 3.1. For the second controller (denoted as Pdf), $\Delta = 0$ for all t. For the last controller (denoted as $Pdf+\Gamma$), the Δ term of (6) is replaced with Γ of (39) [34]

$$\Gamma(t) = \operatorname{sgn}(\dot{\mathbf{x}_{\mathrm{m}}}) \left(k_2 \mathbf{x}_{\mathrm{s}}{}^{\mathsf{T}} \mathbf{x}_{\mathrm{s}} + k_3 \right). \tag{39}$$

For the simulations, the PELICAN robot model presented in [36] and used in [34] is adopted. The simulations are divided into two stages, one of penetration in the medium and another of retreat. The robot starts at a position $q_0 = [45, 135]$ [°] and the medium is at a distance $X_0 = [18.83, 7.62]$ [cm]. For the penetration part of the simulation, consider $A_1 = [33.3, 7.62]$ [cm], which represents a penetration of 15 cm, and $\mathbf{B} = \mathbf{0}$ (passive medium). For the retraction part, $\mathbf{A}$ is switched to $\mathbf{A}_2 = X_0$, which tries to bring the robot to its initial position. Through $\mathbf{A}_1$ and $\mathbf{A}_2$, the interaction of the end effector of the robot with the environment occurs mainly in the x axis, keeping the value of y constant.

The parameters of the controllers are set to $k_2 = 5$ [kg/(m^2 · s)], $k_3 = 5$ [kg/s], $k_{\mathrm{m}} = 10$ [kg/s^2], $g_{\mathrm{h}} = 8$ [kg/s^2], $k_{\mathrm{g}} = 1$ [m/m], $k_{\mathrm{s}} = 15$ [kg/s^2], $k_{\mathrm{f}} = 1$ [N/N], $k_{\mathrm{e}} = 200$, $k_{\alpha 1} = 200$ [kg/s] and $k_{\alpha 2} = 0.1$ [s^3/(kg · m^2)].

The simulation of each control scheme is repeated using three random sinusoidal time delays, with the following maximum values: $\max(h_{\mathrm{low}}) = 100$ [ms], $\max(h_{\mathrm{medium}}) = 500$ [ms] and $\max(h_{\mathrm{high}}) = 1$ [s].

To facilitate the interpretation of the results, $\mathbf{f}_{\mathrm{a_h}} = \mathbf{f}_{\mathrm{a_e}} = \mathbf{0}$ is taken. Conservatively, $K_{\mathrm{h}} = \alpha_{\mathrm{e}} = \alpha_{\mathrm{h}} = 0$, it should

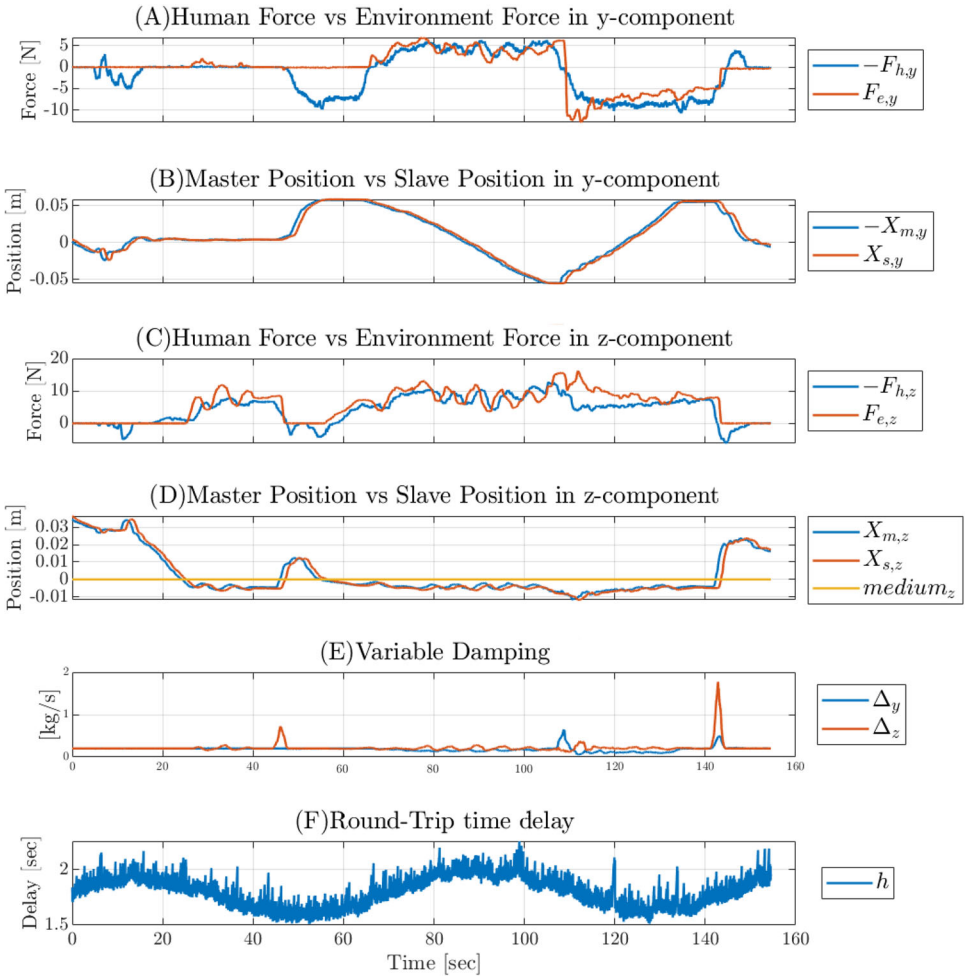

Fig. 7 Experimental results for high delay. **A** Environment-operator force tracking on the y-axis. **B** Environment-operator position tracking on the y-axis. **C** Environment-operator force tracking on the z-axis. **D** Environment-operator position tracking on the z-axis and position of the medium. **E** Evolution of variable damping. **F** Round-trip communication delay

Table 3 Tracking error index

	I_x		I_f		T_{task}
	y-axis	z-axis	y-axis	z-axis	[s]
Low delay	0.0012	0.0009	1.0536	1.3240	117.90
Medium delay	0.0023	0.0013	1.3977	1.4285	148.63
High delay	0.0029	0.0015	2.0694	2.1691	154.50

be noted that values greater than 0 would contribute to the stability of the system.

Figure 8 shows that, given the same parameter settings, all schemes behave similarly, especially for cases where the time delay is high. This is a dual coordination of force and position is achieved. However, the scheme based on explicit nonlinear damping (sign functions in the controller) adds chattering.

Table 4 Qualitative comparison with other studies in the literature

	Operator model	sgn() func	EFC	RFS	DEP	FPS	BEO	BEM
Traditional P+d [14, 22]	Passive + $\mathcal{L}_2$ term	No	No	0	No	No	No	No
Hashemzadeh et al. [33]	LTI	Yes	Yes	1	Yes	Yes	No	No
Mohammadi et al. [34]	Passive + constant force	Yes	No	2	Yes	Yes	No	No
Estrada et al. [40]	Passive + constant force	Yes	No	1	No	Yes	No	No
TDPA based [28–31]	Passive	No	No	0/1	No	Yes	Yes	No
Guajardo-Benavides et al. [35]	$\mathcal{L}_\infty$	Yes	No	0	No	Yes	No	No
Our proposal	Passive + position controller	No	No	2	No	Yes	No	Yes

EFC exogenous force cancellation, *RFS* required force sensors, *DEP* Dependent on Environmental Parameters, *FPS* force position synchronization, *BEO* based on energy observers, *BEM* based on energy measurement

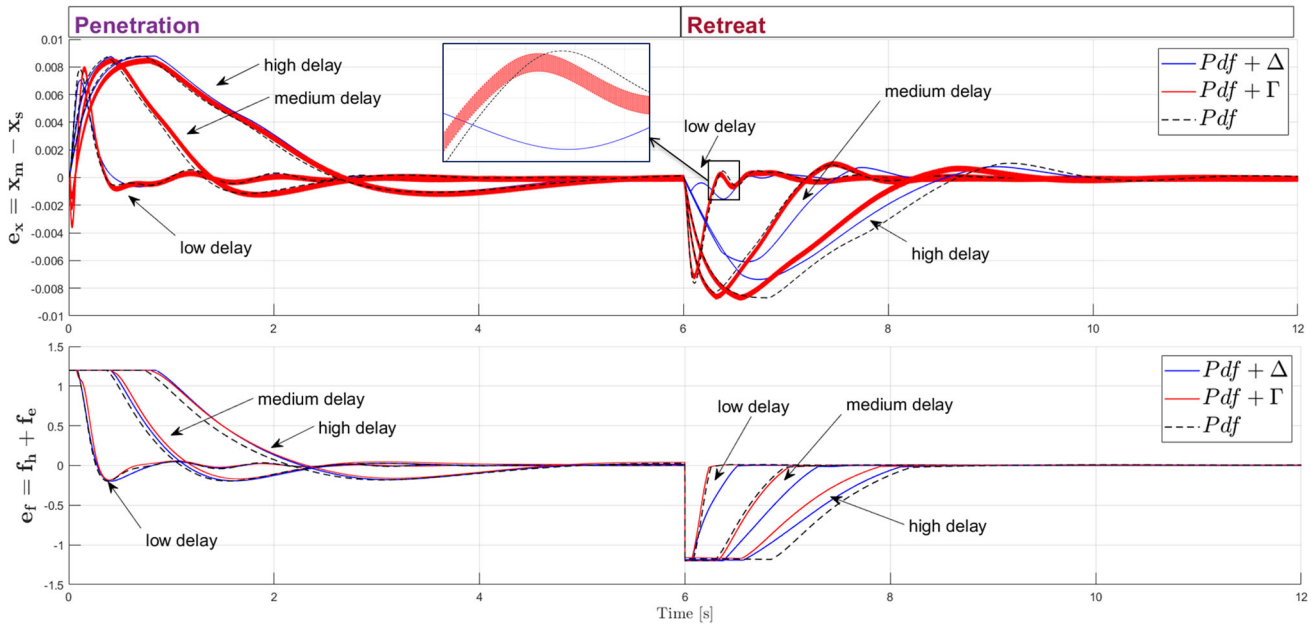

Fig. 8 Position (top) and force (bottom) synchronization errors using Pdf+Δ (blue), Pdf+Γ (red) and Pdf (black) for different time delays: $\max(h_{\text{low}}) = 100$ [ms], $\max(h_{\text{medium}}) = 500$ [ms] and $\max(h_{\text{high}}) = 1$ [s]

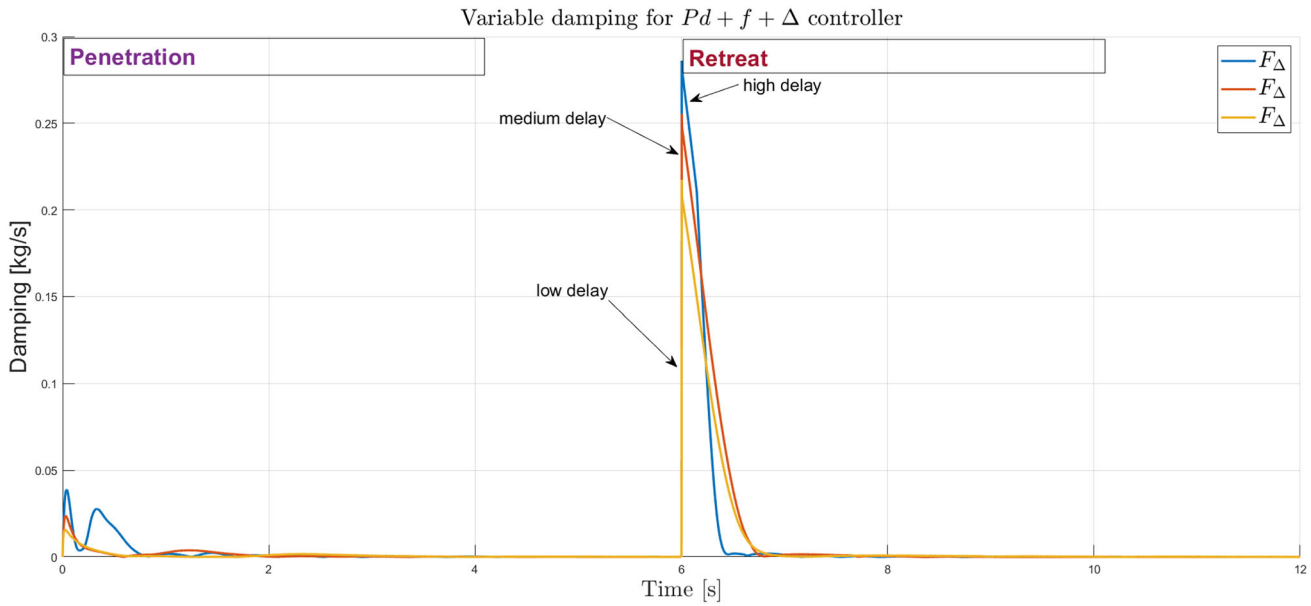

Fig. 9 Force contribution of Δ (F_Δ) in the proposed controller (Pdf+Δ) for different time delays: $\max(h_{\text{low}}) = 100$ [ms] (yellow), $\max(h_{\text{medium}}) = 500$ [ms] (red) and $\max(h_{\text{high}}) = 1$ [s] (blue)

In Fig. 9, it can be seen that the proposed variable damping only acts in the moments of retraction and rebound of the end effector. Although the magnitude of F_Δ increases as the delay increases, its relative magnitude with respect to constant damping gets smaller, and as the speed of movement is also lower, it results in a less evident effect on the total behavior of the system. However, it is observed that the variable damping acts for a short period after retraction (maximum feedback energy) damping the initial effect and subsequently deactivating itself, thus contributing to the signal stabilization time. This behavior can be accentuated by proper parameter settings: tuning $k_{\alpha 1}$, the time during which the variable damping acts can be adjusted, and through $k_{\alpha 2}$ its magnitude.

6 Discussions and conclusions

In this paper, a strategy that considers the effect of time delay has been proposed in order to get a stable bilateral teleoperation of a manipulator robot. It is based on injecting linear damping, avoiding the use of nonlinear damping and dependence on the medium properties, which is impractical. The proposed controller can be applied in commercial robots which generally include PID structures.

The stability theoretical analysis together with the performed simulations give us as a result a general law to qualitatively online calibrate the controller to achieve a stable simultaneous synchronization of position and force, where the injected damping mainly depends on the time delay and feedback power that considers the leader velocity and delayed environment force.

The analysis shows that the system achieves bounded force and position errors regardless of the time delay as well as the elasticity of the medium. Although, as usual in bilateral teleoperation, the environment parameters influence the system performance, the study of this phenomenon for this family of controllers is outside the scope of this work. It is important to remark that the proposed scheme avoids the use of discontinuities in the controller and consequent chattering as well as energy observers are not used. Our proposal requires the use of force sensors and the main limitation at theoretical level is that the analysis presented does not allow assure a convergence of the force and position errors in finite time.

The results of this study contribute to the improvement of the trade-off between stability and transparency, rising and extending the potential use of bilateral teleoperation systems to a broader range of applications.

Author Contributions DDS, ES, LRS and VAM contributed to conceptualization; DDS, ES and LRS provided methodology; DDS and ES performed formal analysis, investigation, and writing—original draft preparation; ES and LRS performed writing—review and editing; ES and VAM contributed to funding acquisition, resources, and supervision.

Funding This work was supported by the National Scientific and Technical Research Council of Argentina (CONICET).

Data availability No datasets were gererated or analysed during the current study.

Declaration

Conflict of interest The authors declare that they have no conflict of interest.

Appendix A

From the functional $V(\mathbf{x}_m, \dot{\mathbf{x}}_\mathbf{m}, k_g\mathbf{x}_m - \mathbf{x}_s, \mathbf{x}_s, \dot{\mathbf{x}}_\mathbf{s}) = V_1 + V_2 + V_3 + V_4$ represented by (14), (15), (16) and (17), remembering that $\mathbf{e} = k_g\mathbf{x}_m - \mathbf{x}_s$; its derivative along the system trajectories will be obtained.

First, the time derivative of (14), including the leader robot dynamics (1)), and Properties 1 and 2, is accomplished as:

$$\begin{aligned}\dot{V}_1 &= \tfrac{1}{2}\dot{\mathbf{x}}_\mathbf{m}^\mathsf{T}\dot{\mathbf{M}}_\mathbf{m}\dot{\mathbf{x}}_\mathbf{m} + \dot{\mathbf{x}}_\mathbf{m}^\mathsf{T}\mathbf{M}_m\ddot{\mathbf{x}}_\mathbf{m} + \kappa_1\dot{\mathbf{x}}_\mathbf{m}^\mathsf{T}\mathbf{x}_m,\\ &= \dot{\mathbf{x}}_\mathbf{m}^\mathsf{T}(\mathbf{f}_h + \mathbf{f}_m - \mathbf{g}_m) + \kappa_1\dot{\mathbf{x}}_\mathbf{m}^\mathsf{T}\mathbf{x}_m + \tfrac{1}{2}\dot{\mathbf{x}}_\mathbf{m}^\mathsf{T}\left(\dot{\mathbf{M}}_\mathbf{m} - 2\mathbf{C}_m\right)\dot{\mathbf{x}}_\mathbf{m},\\ &= \dot{\mathbf{x}}_\mathbf{m}^\mathsf{T}(\mathbf{f}_h + \mathbf{f}_m - \mathbf{g}_m) + \kappa_1\dot{\mathbf{x}}_\mathbf{m}^\mathsf{T}\mathbf{x}_m. \end{aligned} \tag{A.1}$$

Next, if the control action $\mathbf{f}_m$ (6), including the delayed environment force $\mathbf{f}_e$ (3) with $\mathbf{B} = \mathbf{0}$, and the human force $\mathbf{f}_h$ (4), considering $\mathbf{A} = \mathbf{0}$, are included in (A.1), and then adding and grouping terms by convenience, it yields:

$$\begin{aligned}\dot{V}_1 &= -(\alpha_m + \alpha_h + \Delta)\dot{\mathbf{x}}_\mathbf{m}^\mathsf{T}\dot{\mathbf{x}}_\mathbf{m}\\ &\quad - k_m k_g\dot{\mathbf{x}}_\mathbf{m}^\mathsf{T}\mathbf{x}_m + (k_m - g_h)\dot{\mathbf{x}}_\mathbf{m}^\mathsf{T}\mathbf{x}_s(t - h_2)\\ &\quad + \dot{\mathbf{x}}_\mathbf{m}^\mathsf{T}\mathbf{f}_{a_h}\\ &\quad - k_f\dot{\mathbf{x}}_\mathbf{m}^\mathsf{T}\mathbf{f}_e(t - h_2) + (\kappa_1 - k_h)\dot{\mathbf{x}}_\mathbf{m}^\mathsf{T}\mathbf{x}_m,\\ &= -(\alpha_m + \alpha_h + \Delta)\dot{\mathbf{x}}_\mathbf{m}^\mathsf{T}\dot{\mathbf{x}}_\mathbf{m}\\ &\quad - (k_m - g_h)\dot{\mathbf{x}}_\mathbf{m}^\mathsf{T}\mathbf{e}\\ &\quad - (k_m - g_h)\dot{\mathbf{x}}_\mathbf{m}^\mathsf{T}\int_{t-h_2}^{t}\dot{\mathbf{x}}_\mathbf{s}(\xi)\,\mathrm{d}\xi\\ &\quad + \dot{\mathbf{x}}_\mathbf{m}^\mathsf{T}\mathbf{f}_{a_h}\\ &\quad + k_f\dot{\mathbf{x}}_\mathbf{m}^\mathsf{T}\mathbf{f}_e(t - h_2)\\ &\quad - k_g g_h\dot{\mathbf{x}}_\mathbf{m}^\mathsf{T}\mathbf{x}_m + (\kappa_1 - k_h)\dot{\mathbf{x}}_\mathbf{m}^\mathsf{T}\mathbf{x}_m. \end{aligned} \tag{A.2}$$

Now, $\dot{V}_2$ is obtained from (15):

$$\dot{V}_2 = \kappa_2 k_g\mathbf{e}^\mathsf{T}\dot{\mathbf{x}}_\mathbf{m} - \kappa_2\mathbf{e}^\mathsf{T}\dot{\mathbf{x}}_\mathbf{s}. \tag{A.3}$$

Besides, $\dot{V}_3$ from (16) including the follower dynamics (2) as well as the control action $\mathbf{f}_s$ (7) is given by:

$$\dot{V}_3 = \kappa_3\mathbf{x}_\mathbf{s}^\mathsf{T}\dot{\mathbf{x}}_\mathbf{s} + \tfrac{\kappa_4}{2}\dot{\mathbf{x}}_\mathbf{s}^\mathsf{T}\dot{\mathbf{M}}_\mathbf{s}\dot{\mathbf{x}}_\mathbf{s} + \kappa_4\dot{\mathbf{x}}_\mathbf{s}^\mathsf{T}\mathbf{M}_s\ddot{\mathbf{x}}_\mathbf{s},$$

$$
\begin{aligned}
&= \kappa_3 \mathbf{x}_\mathbf{s}^\mathsf{T}\dot{\mathbf{x}}_\mathbf{s} + \kappa_4 \dot{\mathbf{x}}_\mathbf{s}^\mathsf{T}(\mathbf{f}_\mathrm{s} + \mathbf{f}_\mathrm{e} - \mathbf{g}_\mathrm{s}) - \tfrac{1}{2}\kappa_4 \dot{\mathbf{x}}_\mathbf{s}^\mathsf{T}\left(\dot{\mathbf{M}}_\mathbf{s} - 2\mathbf{C}_\mathrm{s}\right)\dot{\mathbf{x}}_\mathbf{s}, \\
&= \kappa_3 \mathbf{x}_\mathbf{s}^\mathsf{T}\dot{\mathbf{x}}_\mathbf{s} + \kappa_4 \dot{\mathbf{x}}_\mathbf{s}^\mathsf{T}(\mathbf{f}_\mathrm{s} + \mathbf{f}_\mathrm{e} - \mathbf{g}_\mathrm{s}), \\
&= \kappa_3 \mathbf{x}_\mathbf{s}^\mathsf{T}\dot{\mathbf{x}}_\mathbf{s} + \kappa_4 \dot{\mathbf{x}}_\mathbf{s}^\mathsf{T}\Big[k_\mathrm{s}(k_\mathrm{g}\mathbf{x}_\mathrm{m}(t-h_1) \\
&\quad - \mathbf{x}_\mathrm{s}) - \alpha_\mathrm{s}\dot{\mathbf{x}}_\mathbf{s} + \tfrac{1}{k_\mathrm{f}}\mathbf{f}_\mathrm{h}(t-h_1) + \mathbf{f}_\mathrm{e}\Big]. \qquad \text{(A.4)}
\end{aligned}
$$

If the environment force $\mathbf{f}_\mathrm{e}$ (3) and the human force $\mathbf{f}_\mathrm{h}$ (4) are inserted into (A.4), and on the result the terms are rearranged, the below expression is reached:

$$
\begin{aligned}
\dot{V}_3 &= \kappa_3 \mathbf{x}_\mathbf{s}^\mathsf{T}\dot{\mathbf{x}}_\mathbf{s} \\
&\quad + \kappa_4 \dot{\mathbf{x}}_\mathbf{s}^\mathsf{T}\Big[k_\mathrm{s}(k_\mathrm{g}\mathbf{x}_\mathrm{m}(t-h_1) - \mathbf{x}_\mathrm{s}) \\
&\quad - \alpha_\mathrm{s}\dot{\mathbf{x}}_\mathbf{s} + (\mathbf{f}_{\mathrm{a}_\mathrm{e}} - k_\mathrm{e}\mathbf{x}_\mathrm{s} - \alpha_\mathrm{e}\dot{\mathbf{x}}_\mathbf{s}) \\
&\quad + \tfrac{1}{k_\mathrm{f}}(\mathbf{f}_{\mathrm{a}_\mathrm{h}}(t-h_1) - g_\mathrm{h}\mathbf{x}_\mathrm{s}(t-h_1-h_2) \\
&\quad - \alpha_\mathrm{h}\dot{\mathbf{x}}_\mathbf{m}(t-h_1))\Big], \\
&\leq -(\alpha_\mathrm{s} + \alpha_\mathrm{e})\kappa_4 \dot{\mathbf{x}}_\mathbf{s}^\mathsf{T}\dot{\mathbf{x}}_\mathbf{s} \\
&\quad + \left(\kappa_3 - \tfrac{g_\mathrm{h}}{k_\mathrm{f}}\kappa_4 - k_\mathrm{e}\kappa_4\right)\dot{\mathbf{x}}_\mathbf{s}^\mathsf{T}\mathbf{x}_\mathrm{s} \\
&\quad + \tfrac{1}{k_\mathrm{f}}\kappa_4 \dot{\mathbf{x}}_\mathbf{s}^\mathsf{T}\mathbf{f}_{\mathrm{a}_\mathrm{h}}(t-h_1) \\
&\quad + k_\mathrm{s}\kappa_4 \dot{\mathbf{x}}_\mathbf{s}^\mathsf{T}\mathbf{e} - \kappa_4 \dot{\mathbf{x}}_\mathbf{s}^\mathsf{T}\mathbf{f}_{\mathrm{a}_\mathrm{e}} \\
&\quad - k_\mathrm{s}k_\mathrm{g}\kappa_4 \dot{\mathbf{x}}_\mathbf{s}^\mathsf{T}\int_{t-h_1}^{t}\dot{\mathbf{x}}_\mathbf{m}(\xi)\,\mathrm{d}\xi \\
&\quad + \tfrac{g_\mathrm{h}}{k_\mathrm{f}}\kappa_4 \dot{\mathbf{x}}_\mathbf{s}^\mathsf{T}\int_{t-h_1-h_2}^{t}\dot{\mathbf{x}}_\mathbf{s}(\xi)\,\mathrm{d}\xi \\
&\quad + \tfrac{1}{4}\alpha_\mathrm{h}\kappa_4 \dot{\mathbf{x}}_\mathbf{s}^\mathsf{T}\dot{\mathbf{x}}_\mathbf{s} \\
&\quad + \tfrac{1}{4}\alpha_\mathrm{h}\kappa_4 \dot{\mathbf{x}}_\mathbf{m}(t-h_1)^\mathsf{T}\dot{\mathbf{x}}_\mathbf{m}(t-h_1). \qquad \text{(A.5)}
\end{aligned}
$$

Stability analysis is hard to complete because there are terms with delayed variables in (A.2) and (A.5). To solve this, V_4 (17) has been proposed, whose derivative considering Assumption 1 is obtained by:

$$
\begin{aligned}
\dot{V}_4 &\leq \bar{h}_2 \dot{\mathbf{x}}_\mathbf{s}^\mathsf{T}\dot{\mathbf{x}}_\mathbf{s} - \int_{t-h_2}^{t}\dot{\mathbf{x}}_\mathbf{s}^\mathsf{T}(\xi)\dot{\mathbf{x}}_\mathbf{s}(\xi)\,\mathrm{d}\xi \\
&\quad + \kappa_4 \bar{h}_1 \dot{\mathbf{x}}_\mathbf{m}^\mathsf{T}\dot{\mathbf{x}}_\mathbf{m} - \kappa_4 \int_{t-h_1}^{t}\dot{\mathbf{x}}_\mathbf{m}^\mathsf{T}(\xi)\dot{\mathbf{x}}_\mathbf{m}(\xi)\,\mathrm{d}\xi \\
&\quad + \kappa_4\left(\bar{h}_1 + \bar{h}_2\right)\dot{\mathbf{x}}_\mathbf{s}^\mathsf{T}\dot{\mathbf{x}}_\mathbf{s} - \kappa_4 \int_{t-h_1-h_2}^{t}\dot{\mathbf{x}}_\mathbf{s}^\mathsf{T}(\xi)\dot{\mathbf{x}}_\mathbf{s}(\xi)\,\mathrm{d}\xi \\
&\quad + \frac{1}{4}\frac{\kappa_4\alpha_\mathrm{h}}{1-\tau}\dot{\mathbf{x}}_\mathbf{m}^\mathsf{T}\dot{\mathbf{x}}_\mathbf{m} \\
&\quad - \frac{1}{4}\frac{\kappa_4\alpha_\mathrm{h}(1-\dot{h}_1)}{1-\tau}\dot{\mathbf{x}}_\mathbf{m}(t-h_1)^\mathsf{T}\dot{\mathbf{x}}_\mathbf{m}(t-h_1). \qquad \text{(A.6)}
\end{aligned}
$$

The integral terms in (A.6) can be linked with others of (A.2) and (A.5) using Lemma 2 (5), yielding the following relations:

$$
\begin{aligned}
&-(k_\mathrm{m} - g_\mathrm{h})\dot{\mathbf{x}}_\mathbf{m}^\mathsf{T}\int_{t-h_2}^{t}\dot{\mathbf{x}}_\mathbf{s}(\xi)\,\mathrm{d}\xi \\
&\quad - \int_{t-h_2}^{t}\dot{\mathbf{x}}_\mathbf{s}^\mathsf{T}(\xi)\dot{\mathbf{x}}_\mathbf{s}(\xi)\,\mathrm{d}\xi \\
&\leq \tfrac{1}{4}\bar{h}_2(k_\mathrm{m} - g_\mathrm{h})^2 \dot{\mathbf{x}}_\mathbf{m}^\mathsf{T}\dot{\mathbf{x}}_\mathbf{m} \qquad \text{(A.7)} \\
&-k_\mathrm{s}k_\mathrm{g}\kappa_4 \dot{\mathbf{x}}_\mathbf{s}^\mathsf{T}\int_{t-h_1}^{t}\dot{\mathbf{x}}_\mathbf{m}(\xi)\,\mathrm{d}\xi \\
&\quad -\kappa_4\int_{t-h_1}^{t}\dot{\mathbf{x}}_\mathbf{m}^\mathsf{T}(\xi)\dot{\mathbf{x}}_\mathbf{m}(\xi)\,\mathrm{d}\xi \\
&\quad \leq \tfrac{1}{4}\bar{h}_1(k_\mathrm{s}k_\mathrm{g})^2\kappa_4 \dot{\mathbf{x}}_\mathbf{s}^\mathsf{T}\dot{\mathbf{x}}_\mathbf{s} \qquad \text{(A.8)}
\end{aligned}
$$

$$
\begin{aligned}
&\tfrac{g_\mathrm{h}}{k_\mathrm{f}}\kappa_4 \dot{\mathbf{x}}_\mathbf{s}^\mathsf{T}\int_{t-h_1-h_2}^{t}\dot{\mathbf{x}}_\mathbf{s}(\xi)\,\mathrm{d}\xi \\
&-\kappa_4\int_{t-h_1-h_2}^{t}\dot{\mathbf{x}}_\mathbf{s}^\mathsf{T}(\xi)\dot{\mathbf{x}}_\mathbf{s}(\xi)\,\mathrm{d}\xi \leq \tfrac{1}{4}(\bar{h}_1 \\
&\quad + \bar{h}_2)\left(\tfrac{g_\mathrm{h}}{k_\mathrm{f}}\right)^2\kappa_4 \dot{\mathbf{x}}_\mathbf{s}^\mathsf{T}\dot{\mathbf{x}}_\mathbf{s} \qquad \text{(A.9)}
\end{aligned}
$$

Finally, $\dot{V}$ can be built joining equations (A.1)–(A.6), considering the relations given by (A.7)–(A.9) to avoid terms with integrals, knowing that the negative last term of (A.6) always overcome the last term of (A.5) according to Assumption 1, and defining constants κ_i as $\kappa_1 = k_\mathrm{g}g_\mathrm{h} + k_\mathrm{h}$, $\kappa_2 = (k_\mathrm{m} - g_\mathrm{h})/k_\mathrm{g}$, $\kappa_3 = \kappa_4(g_\mathrm{h}/k_\mathrm{f} + k_\mathrm{e})$ and $\kappa_4 = \kappa_2/k_\mathrm{s}$ in order to cancel all opposing terms. The final relation obtained to represent $\dot{V}$ is given by:

$$
\begin{aligned}
\dot{V} &= \dot{V}_1 + \dot{V}_2 + \dot{V}_3 + \dot{V}_4 \\
&\leq -\Big[(\alpha_\mathrm{m} + \Delta) + \left(1 - \tfrac{\kappa_4}{4(1-\tau)}\right)\alpha_\mathrm{h} - \kappa_4\bar{h}_1 \\
&\quad - \tfrac{1}{4}(k_\mathrm{m} - g_\mathrm{h})^2\bar{h}_2\Big]\dot{\mathbf{x}}_\mathbf{m}^\mathsf{T}\dot{\mathbf{x}}_\mathbf{m} \\
&\quad - \kappa_4\Big[(\alpha_\mathrm{s} + \alpha_\mathrm{e}) - \left(1 + \left(\tfrac{k_\mathrm{s}k_\mathrm{g}}{2}\right)^2\right. \\
&\quad + \left.\left(\tfrac{g_\mathrm{h}}{2k_\mathrm{f}}\right)^2\right)\bar{h}_1 - \left(1 + \tfrac{1}{\kappa_4}\right. \\
&\quad + \left.\left(\tfrac{g_\mathrm{h}}{2k_\mathrm{f}}\right)^2\right)\bar{h}_2\Big]\dot{\mathbf{x}}_\mathbf{s}^\mathsf{T}\dot{\mathbf{x}}_\mathbf{s} \\
&\quad - k_\mathrm{f}\dot{\mathbf{x}}_\mathbf{m}^\mathsf{T}\mathbf{f}_\mathrm{e}(t-h_2) \\
&\quad + \dot{\mathbf{x}}_\mathbf{m}^\mathsf{T}\mathbf{f}_{\mathrm{a}_\mathrm{h}} \\
&\quad + \kappa_4 \dot{\mathbf{x}}_\mathbf{s}^\mathsf{T}\left(\tfrac{1}{k_\mathrm{f}}\mathbf{f}_{\mathrm{a}_\mathrm{h}}(t-h_1) + \mathbf{f}_{\mathrm{a}_\mathrm{e}}\right) \qquad \text{(A.10)}
\end{aligned}
$$

The result achieved in (A.10) is used to complete the stability and convergence analysis of force and position signals of the leader–follower teleoperation system.

References

1. Sheridan TB (1992) Telerobotics, automation, and human supervisory control. MIT Press, Cambridge
2. Antonakoglou K, Xu X, Steinbach E, Mahmoodi T, Dohler M (2018) Toward haptic communications over the 5G tactile internet. IEEE Commun Surv Tuts 20(4):3034–3059
3. Hokayem PF, Spong MW (2006) Bilateral teleoperation: an historical survey. Automatica 42(12):2035–2057
4. Richard JP (2003) Time-delay systems: an overview of some recent advances and open problems. Automatica 39(10):1667–1694
5. Sipahi R, Niculescu S-I, Abdallah CT, Michiels W, Gu K (2011) Stability and stabilization of systems with time delay. IEEE Control Syst Mag 31(1):38–65
6. Slawiñski E, Mut V, Santiago D (2016) Pd-like controller for delayed bilateral teleoperation of wheeled robots. Int J Control 89(8):1622–1631
7. Farkhatdinov I, Ryu J-H, Poduraev J (2008) A feasibility study of time-domain passivity approach for bilateral teleoperation of mobile manipulator. In: Proceedings of the IEEE international conference on control, automation and systems, pp 272– 277
8. Santiago DD, Slawiñski E, Mut VA (2017) Stable delayed bilateral teleoperation of mobile manipulators. Asian J Control 19(3):1140–1152
9. Xu G-H, Qi F, Lai Q, Iu HH-C (2020) Fixed time synchronization control for bilateral teleoperation mobile manipulator with nonholonomic constraint and time delay. IEEE Trans Circuits Syst II 67(12):3452–3456
10. Slawiñski E, Santiago D, Mut V (2017) Control for delayed bilateral teleoperation of a quadrotor. ISA Trans 71:415–425
11. Lam T, Mulder M, Van Paassen M (2008) Haptic feedback in uninhabited aerial vehicle teleoperation with time delay. J Guid Control Dyn 31(6):1728–1739
12. Zhao X-W, Han G, Lai Q, Yue D (2020) Multiconsensus of first-order multiagent systems with directed topologies. Mod Phys Lett B 34(23):2050240
13. Nuno E, Sarras I, Basanez L (2013) Consensus in networks of nonidentical Euler–Lagrange systems using P+d controllers. IEEE Trans Robot 29(6):1503–1508
14. Nuño E, Basañez L, Ortega R (2011) Passivity-based control for bilateral teleoperation: a tutorial. Automatica 47(3):485–495
15. Anderson RJ, Spong MW (1989) Bilateral control of teleoperators with time delay. IEEE Trans Autom Control 34(5):494–501
16. Niemeyer G, Slotline J (1991) Stable adaptive teleoperation. IEEE J Ocean Eng 16(1):152–162
17. Lee D, Huang K (2010) Passive-set-position-modulation framework for interactive robotic systems. IEEE Trans Robot 26(2):354–369
18. Nuño E, Ortega R, Barabanov N, Basañez L (2008) A globally stable PD controller for bilateral teleoperators. IEEE Trans Robot 24(3):753–758
19. Cho HC, Park JH (2005) Stable bilateral teleoperation under a time delay using a robust impedance control. Mechatronics 15(5):611–625
20. Li Y, Yin Y, Zhang D (2018) Adaptive task-space synchronization control of bilateral teleoperation systems with uncertain parameters and communication delays. IEEE Access 6:5740–5748
21. Dyck M, Jazayeri A, Tavakoli M (2013) Is the human operator in a teleoperation system passive? In: World haptics conference (WHC). IEEE, Daejeon, pp 683–688
22. Hua C-C, Liu XP (2010) Delay-dependent stability criteria of teleoperation systems with asymmetric time-varying delays. IEEE Trans Robot 26(5):925–932
23. Islam S, Liu XP, El Saddik A (2013) Teleoperation systems with symmetric and unsymmetric time varying communication delay. IEEE Trans Instrum Meas 62(11):2943–2953
24. Li H, Zhang L, Kawashima K (2018) Operator dynamics for stability condition in haptic and teleoperation system: a survey. Int J Med Robot Comput Assist Surg 14(2):1881
25. Lawrence DA (1993) Stability and transparency in bilateral teleoperation. IEEE Trans Robot Autom 9(5):624–637
26. Slawiñski E, Mut VA, Fiorini P, Salinas LR (2012) Quantitative absolute transparency for bilateral teleoperation of mobile robots. IEEE Trans Syst Man Cybern A 42(2):430–442
27. Shahbazi M, Atashzar SF, Tavakoli M, Patel RV (2018) Position-force domain passivity of the human arm in telerobotic systems. IEEE/ASME Trans Mechatron 23(2):552–562
28. Singh H, Panzirsch M, Coelho A, Ott C (2020) Proxy-based approach for position synchronization of delayed robot coupling without sacrificing performance. IEEE Robot Autom Lett 5(4):6599–6606
29. Chawda V, O'Malley MK (2014) Position synchronization in bilateral teleoperation under time-varying communication delays. IEEE/ASME Trans Mechatron 20(1):245–253
30. Panzirsch M, Pereira A, Singh H, Weber B, Ferreira E, Gherghescu A, Hann L, Exter E, Hulst F, Gerdes L et al (2022) Exploring planet geology through force-feedback telemanipulation from orbit. Sci Robot 7(65):6307
31. Ryu J-H, Artigas J, Preusche C (2010) A passive bilateral control scheme for a teleoperator with time-varying communication delay. Mechatronics 20(7):812–823
32. Franken M, Stramigioli S, Misra S, Secchi C, Macchelli A (2011) Bilateral telemanipulation with time delays: a two-layer approach combining passivity and transparency. IEEE Trans Robot 27(4):741–756
33. Hashemzadeh F, Tavakoli M (2015) Position and force tracking in nonlinear teleoperation systems under varying delays. Robotica 33(4):1003–1016
34. Mohammadi K, Talebi HA, Zareinejad M (2016) A novel position and force coordination approach in four channel nonlinear teleoperation. Comput Electr Eng 56:688–699
35. Guajardo-Benavides EJ, Arteaga MA (2023) On the finite time force estimation for bilateral teleoperation of robot manipulators with time varying delays. Control Eng Pract 138:105622
36. Kelly R, Davila VS, Perez JAL (2006) Control of robot manipulators in joint space. Springer, London
37. Slawiñski E, Moya V, Santiago D, Mut V (2019) Force and position-velocity coordination for delayed bilateral teleoperation of a mobile robot. Robotica 37(10):1768–1784
38. Hou M, Duan G, Guo M (2010) New versions of Barbalat's lemma with applications. J Control Theory Appl 8(4):545–547
39. Hua C, Liu PX (2009) Delay-dependent stability analysis of teleoperation systems with unsymmetric time-varying delays. In: Proceedings of IEEE international conference on robotics and automation, pp 1146–1151
40. Estrada E, Yu W, Li X (2019) Stability and transparency of delayed bilateral teleoperation with haptic feedback. Int J Appl Math Comput Sci 29(4):681–692